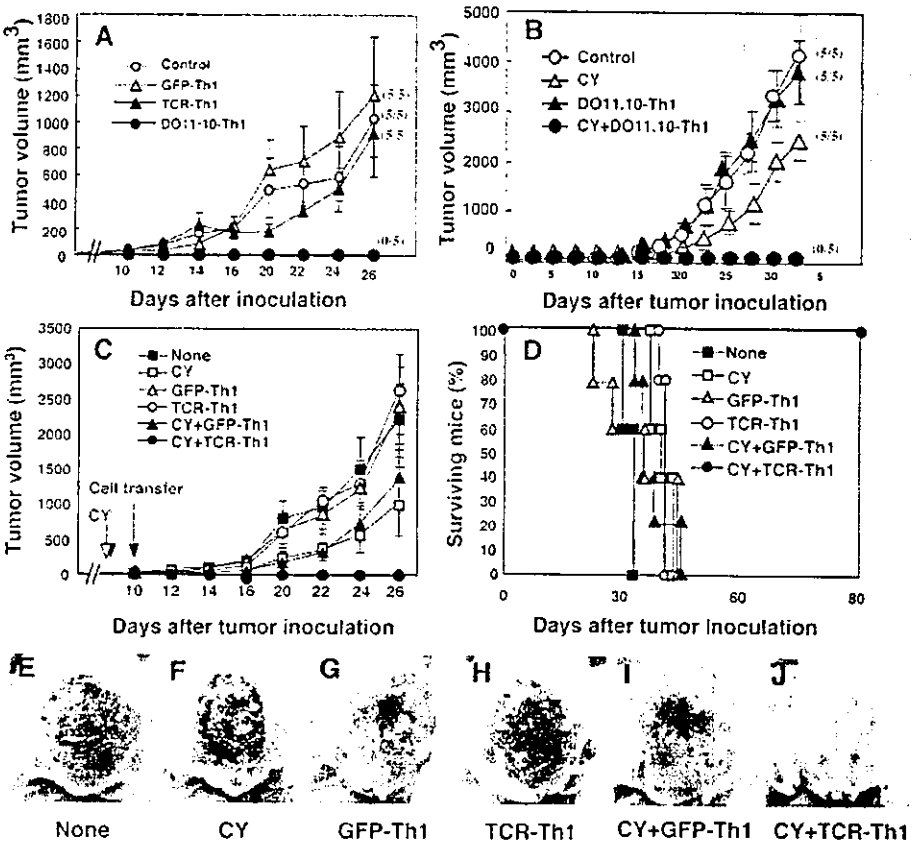

Fig. 4. T-cell receptor (*TCR*)-transduced artificial T-helper type 1 (*Th1*) cells, in combination with cyclophosphamide (*CY*) treatment, eradicate established tumors. A20-OVA cells (2×10^6) were intradermally inoculated into BALB/c mice. When the tumor mass became palpable (6–8 mm), the tumor-bearing mice were treated with various protocols. *A*, tumor-bearing mice were treated with none (○) or cell transfer (2×10^7/mouse) of DO11.10-Th1 (●), TCR-Th1 (▲) or green fluorescent protein (*GFP*)-Th1 cells (△). *B*, tumor-bearing mice were transferred with none (○), CY (△), DO11.10-Th1 (▲) or CY plus DO11.10-Th1 (●). Th1 cells (5×10^6) were transferred into tumor-bearing mice 24 h after CY (80 mg/kg) treatment. *C–J*, tumor-bearing mice were treated with none (■ in *C* and *D*; *photo E*), CY (□ in *C* and *D*; *photo F*), mock GFP-transduced Th1 cells (△ in *C* and *D*; photo G), TCR-transduced Th1 cells (○ in *C* and *D*; *photo H*), CY + mock GFP-transduced Th1 cells (▲ in *C* and *D*; *photo I*) or CY + TCR-Th1 cells (● in *C* and *D*; *photo J*). In experiments shown in *C–D*, Th1 cells (5×10^6 cells/mouse) were i.v. transferred into tumor-bearing mice 1 day after i.p. injection of CY (80 mg/kg). The antitumor activity mediated by the transferred cells was determined by measuring tumor size in perpendicular diameters. Tumor volume was calculated as described in "Materials and Methods." The *fractional numbers in parentheses* in *A* and *B*, dead mice/total mice within 60 days after tumor inoculation. The *bars*, mean ± SE of five mice in each experimental group. Similar results were obtained in three separate experiments.

CY might be better to induce the efficient therapeutic effect of genetically modified Th1 cells, although the transfer of large numbers of TCR-transduced Th1 cells might be effective. CY treatment alone or combined therapy with mock-transduced Th1 cells and CY failed to cure tumor-bearing mice, although these treatments showed a slight inhibition of tumor growth *in vivo*. Such antitumor activity by combination therapy with TCR-transduced Th1 cells and CY was not observed in A20 tumor-bearing mice (data not shown). Thus, these results clearly demonstrate that TCR-transduced Th1 cells induced from nonspecific Th1 cells exhibit specific antitumor activity *in vivo*. That combination therapy with TCR-transduced Th1 and CY can induce immunological memory *in vivo* was indicated by the fact that (*a*) all cured mice by treatment with TCR-transduced Th1 cells and CY could reject rechallenged A20-OVA tumor cells and (*b*) $CD8^+$ and $CD4^+$ CTLs were demonstrated in cured mice.[4]

Recently, $CD4^+$ T cells were demonstrated to play a crucial role not only in the induction of $CD8^+$ CTLs via dendritic cell activation (14–16) but also for maintaining the number and function of CTLs (14–18). Coadministration of $CD4^+$ T cells with $CD8^+$ T cells resulted in increased CTL activity and enhanced infiltration of these cells into tumors; both facilitate CTL-mediated tumor eradication *in vivo* (19). The rationale for introducing $CD4^+$ T-cell help for promoting antitumor immunity is supported by the fact that $CD4^+$ T cells augment the therapeutic effect of tumor vaccines that are based on MHC class I-binding peptides or dendritic cells (19). An important role for $CD4^+$ T-cell help has also been reported in tumor chemotherapy using CY (20). CY, in addition to its direct antitumoricidal activities, appears to act as an immunomodulator that facilitates the generation of antitumor effector T cells combined with $CD4^+$ T-cell help.

In a prior report (6), we demonstrated that adoptive cell transfer of a large number ($>2 \times 10^7$ cells) of Th1 cells is beneficial for inducing tumor-specific CTLs *in vivo* and for curing mice of established tumors. However, adoptive transfer of $<10^7$ Th1 cells was insufficient to cure tumor-bearing mice. This Th1-dependent antitumor immunity is completely dependent on the generation of host-derived tumor-specific CTL, because Th1 cell-therapy was unable to eradicate tumors in RAG-$2^{-/-}$ mice unless $CD8^+$ T cells were cotransferred. Therefore, when adoptive immunotherapy using Th1 cells was combined with dendritic cell-based tumor vaccine therapy that promotes CTL generation, the number of required Th1 cells decreased to 5×10^6 cells per mouse (19). Here, we further demonstrate that the therapeutic effect of CY is greatly augmented by combination therapy with a small number (5×10^6) of TCR-transduced Th1 cells as well as DO11.10-derived Th1 cells (Fig. 4). The immunopotentiating mechanisms of CY remains unclear, but CY treatment appeared to enhance the migration of Th1 cells into tumor local site including draining lymph node.[4] Then, the transferred Th1 cells exhibited proliferation and cytokine production by interacting with APC, which processed antigen of tumor cells destroyed by CY and/or Th1 cells. Thus, transferred Th1 cells introduce tumor local help that is essential for generating tumor-specific CTLs to eradicate established tumor.

The strategy used here for promoting tumor antigen-specific Th1 responses holds significant promise for tumor immunotherapy in human patients. A number of human tumor-antigen-specific T cells have been established. For example, several Th clones reactive against the class II-binding tumor rejection antigen peptide have been established (21–24). We have already cloned the TCR genes from a tumor-specific Th cell clone and introduced the TCR gene into polyclonally activated human T cells. These transduced T cells were able to produce cytokines in response to the relevant antigen.[4] These findings illustrate the feasibility of applying antigen-specific Th1 cells

to adoptive tumor immunotherapy, either by inducing tumor-specific Th1 cells from patient samples or by TCR transduction, as described here.

Th1-dominant immunity plays a critical role in the induction of antitumor immunity at the local tumor site via multiple helper functions such as their capacity to enhance CTL priming of APC and to promote migration, proliferation, and cytotoxicity of tumor-specific CTLs (14–19, 25–27). Therefore, adoptive immunotherapy using tumor-specific Th1 cells combined with other therapeutic modalities such as (*a*) dendritic cell-based tumor vaccine therapy; (*b*) $CD8^+$ T-cell therapy; (*c*) chemotherapy; or (*d*) radiation therapy (28, 29), may provide a more efficient strategy for tumor immunotherapy. Our protocol for inducing TCR-transduced tumor-specific Th1 cells should enable us to prepare tumor-specific Th1 cells even when tumor-specific Th1 cells from the patient cannot be obtained. This strategy should prove valuable for developing effective tumor immunotherapies. For application to clinical trial, the use of TCR-transduced Th1 cells comodified with thymidine kinase (TK) gene might be better strategy to prevent unwanted immune disorders induced by long-lived transferred Th1 cells (30).

ACKNOWLEDGMENTS

We thank Dr. Luc Van Kaer (Vanderbilt University School of Medicine, Nashville, TN) for reviewing this paper. We also thank Dr. Michiko Kobayashi (Genetics Institute, Cambridge, MA) and Takuko Sawada (Shionogi Pharmaceutical Institute Co., Osaka, Japan) for their kind donations of IL-12 and IL-2, respectively.

REFERENCES

1. Trinchieri, G. Interleukin-12 and the regulation of innate resistance and adaptive immunity. Nat. Rev. Immunol., *3:* 133–146, 2003.
2. Nishimura, T., Nakui, M., Sato, M., Iwakabe, K., Kitamura, H., Sekimoto, M., Ota, A., Koda, T., and Nishimura, S. The critical role of Th1-dominant immunity in tumor immunology. Cancer Chemother. Pharmacol., *46:* S52–S61, 2000.
3. Tada, T., Ohzeki, S., Utsumi, K., Takiuchi, H., Muramatsu, M., Li, X. F., Shimizu, J., Fujiwara, H., and Hamaoka, T. Transforming growth factor-β-induced inhibition of T cell function. Susceptibility difference in T cells of various phenotypes and functions and its relevance to immunosuppression in the tumor-bearing state. J. Immunol., *146:* 1077–1082, 1991.
4. Sakaguchi, S., Sakaguchi, N., Shimizu, J., Yamazaki, S., Sakihama, T., Itoh, M., Kuniyasu, Y., Nomura, T., Toda, M., and Takahashi, T. Immunologic tolerance maintained by $CD25^+$ $CD4^+$ regulatory T cells: their common role in controlling autoimmunity, tumor immunity, and transplantation tolerance. Immunol. Rev., *182:* 18–32, 2001.
5. Kobie, J. J., Wu, R. S., Kurt, R. A., Lou, S., Adelman, M. K., Whitesell, L. J., Ramanathapuram, L. V., Arteaga, C. L., and Akporiaye, E. T. Transforming growth factor β inhibits the antigen-presenting functions and antitumor activity of dendritic cell vaccines. Cancer Res., *63:* 1860–1864, 2003.
6. Nishimura, T., Iwakabe, K., Sekimoto, M., Ohmi, Y., Yahata, T., Nakui, M., Sato, T., Habu, S., Tashiro, H., Sato, M., and Ohta, A. Distinct role of antigen-specific T helper type 1 (Th1) and Th2 cells in tumor eradication *in vivo*. J. Exp. Med., *190:* 617–627, 1999.
7. Fujio, K., Misaki, Y., Setoguchi, K., Morita, S., Kawahata, K., Kato, I., Nosaka, T., Yamamoto, K., and Kitamura, T. Functional reconstitution of class II MHC-restricted T cell immunity mediated by retroviral transfer of the $\alpha\beta$ TCR complex. J. Immunol., *165:* 528–532, 2000.
8. Kessels, H. W., Wolkers, M. C., Van den Boom, M. D., Van der Valk, M. A., and Schumacher, T. N. Immunotherapy through TCR gene transfer. Nat. Immunol., *2:* 957–961, 2001.
9. Stanislawski, T., Voss, R. H., Lotz, C., Sadovnikova, E., Willemsen, R. A., Kuball, J., Ruppert, T., Bolhuis, R. L., Melief, C. J., Huber, C., Stauss, H. J., and Theobald, M. Circumventing tolerance to a human MDM2-derived tumor antigen by TCR gene transfer. Nat Immunol., *2:* 962–970, 2001.
10. Tsuji, T., Chamoto, K., Funamoto, H., Kosaka, A., Matsuzaki, J., Abe, H., Fujio, K., Yamamoto, K., Kitamura, T., Togashi, Y., Koda, T., and Nishimura, T. An efficient method to prepare T cell receptor gene-transduced cytotoxic T lymphocytes type 1 applicable to tumor gene cell-therapy. Cancer Sci., *94:* 389–393, 2003.
11. Nishimura, T., Burakoff, S. J., and Herrmann, S. H. Protein kinase C required for cytotoxic T lymphocyte triggering. J. Immunol., *139:* 2888–2891, 1987.
12. Ohta, S., Tsukamoto, H., Watanabe, K., Makino, K., Kuge, S. Hanai, N., Habu, S., and Nishimura, T. Tumor-associated glycoantigen, sialyl Lewis(a) as a target for bispecific antibody-directed adoptive tumor immunotherapy. Immunol. Lett., *44:* 35–40, 1995.
13. Indraccolo, S., Habeler, W., Tisato, V., Stievano, L., Piovan, E., Toscllo, V., Esposito, G., Wagner, R., Uberla, K., Chieco-Bianchi, L., and Amadori, A. Gene transfer in ovarian cancer cells: a comparison between retroviral and lentiviral vectors. Cancer Res., *62:* 6099–6107, 2002.
14. Bennett, S. R., Carbone, R. F., Karamalis, F., Flavell, R. A., Miller, J. F., and Heath, W. R. Help for cytotoxic-T-cell responses is mediated by CD40 signalling. Nature (Lond.), *393:* 478–480, 1998.
15. Schoenberger, S. P., Toes, R. E., Van. der Voort, E. I., Offringa, R., and Melief, C. J. T-cell help for cytotoxic T lymphocytes is mediated by CD40-CD40L interactions. Nature (Lond.), *393:* 480–483, 1998.
16. Ridge, J. P., Di Rosa, F., and Matzinger, P. A conditioned dendritic cell can be a temporal bridge between a $CD4^+$ T-helper and a T-killer cell. Nature (Lond.), *393:* 474–478, 1998.
17. Marzo, A. L., Kinnear, B. F., Lake, R. A., Frelinger, J. J., Collins, E. J., Robinson, B. W., and Scott, B. Tumor-specific $CD4^+$ T cells have a major "post-licensing" role in CTL mediated anti-tumor immunity. J. Immunol., *165:* 6047–6055, 2000.
18. Yu, P., Spiotto, M. T., Lee, Y., Schreiber, H., and Fu, Y. X. Complementary role of $CD4^+$ T cells and secondary lymphoid tissues for cross-presentation of tumor antigen to $CD8^+$ T cells. J. Exp. Med., *197:* 985–995, 2003.
19. Sato, M., Chamoto, K., and Nishimura T. A novel tumor-vaccine cell therapy using bone marrow-derived dendritic cell type 1 and antigen-specific Th1 cells. Int. Immunol., *15:* 837–843, 2003.
20. Saxton, M. L., Longo, D. L., Wetzel, H. E., Tribble, H., Alvord, W. G., Kwak, L. W., Leonard, A. S., Ullmann, C. D., Curti, B. D., and Ochoa, A. C. Adoptive transfer of anti-CD3-activated $CD4^+$ T cells plus cyclophosphamide and liposome-encapsulated interleukin-2 cure murine MC-38 and 3LL tumors and establish tumor-specific immunity. Blood, *89:* 2529–2536, 1997.
21. Kobayashi, H., Song, Y., Hoon, D. S., Appella, E., and Celis, E. Tumor-reactive T helper lymphocytes recognize a promiscuous MAGE-A3 epitope presented by various major histocompatibility complex class II alleles. Cancer Res., *61:* 4773–4778, 2001.
22. Zarour, H. M., Maillere, B., Brusic, V., Coval, K., Williams, E., Pouvelle-Moratille, S., Castelli, F., Land, S., Bennouna, J., Logan, T., and Kirkwood, J. M. NY-ESO-1 119-143 is a promiscuous major histocompatibility complex class II T-helper epitope recognized by Th1- and Th2-type tumor-reactive $CD4^+$ T cells. Cancer Res., *62:* 213–218, 2002.
23. Kobayashi, H., Omiya, R., Ruiz, M., Huarte, E., Sarobe, P., Lasarte, J. J., Herraiz, J., Sangro, B., Prieto, J., Borras-Cuesta, F., and Celis, E. Identification of an antigenic epitope for helper T lymphocytes from carcinoembryonic antigen. Clin. Cancer Res., *8:* 3219–3225, 2002.
24. Tatsumi, T., Kierstead, L. S., Ranieri, E., Gesualdo, L., Schena, F. P., Finke, J. H., Bukowski, R. M., Mueller-Berghaus, J., Kirkwood, J. M., Kwok, W. W., and Storkus, W. J. Disease-associated bias in T helper type 1 (Th1)/Th2 CD4(+) T cell responses against MAGE-6 in HLA-DRB10401(+) patients with renal cell carcinoma or melanoma. J. Exp. Med., *196:* 619–628, 2002.
25. Giuntoli, R. L., II, Lu, J., Kobayashi, H., Kennedy, R., and Celis, E. Direct costimulation of tumor-reactive CTL by helper T cells potentiate their proliferation, survival, and effector function. Clin. Cancer Res., *8:* 922–931, 2002.
26. Nakajima, C., Uekusa, Y., Iwasaki, M., Yamaguchi, N., Mukai, T., Gao, P., Tomura, M., Ono, S., Tsujimura, T., Fujiwara, H., and Hamaoka, T. A role of interferon-γ (IFN-γ) in tumor immunity: T cells with the capacity to reject tumor cells are generated but fail to migrate to tumor sites in IFN-γ-deficient mice. Cancer Res., *61:* 3399–3405, 2001.
27. Uekusa, Y., Gao, P., Yamaguchi, N., Tomura, M., Mukai, T., Nakajima, C., Iwasaki, M., Takeuchi, N., Tsujimura, T., Nakazawa, M., Fujiwara, H., and Hamaoka, T. A role for endogenous IL-12 in tumor immunity: IL-12 is required for the acquisition of tumor-migratory capacity by T cells and the development of T cell-accepting capacity in tumor masses. J. Leukoc. Biol., *72:* 864–873, 2002.
28. Plautz, G. E., Inoue, M., and Shu, S. Defining the synergistic effects of irradiation and T-cell immunotherapy for murine intracranial tumors. Cell. Immunol., *171:* 277–284, 1996.
29. Ganss, R., Ryschich, E., Klar, E., Arnold, B., and Hammerling, G. J. Combination of T-cell therapy and trigger of inflammation induce remodeling of the vasculature and tumor eradication. Cancer Res., *62:* 1462–1470, 2002.
30. Mesnil, M., and Yamasaki, H. Bystander effect in herpes simplex virus-thymidine kinase/ganciclovir cancer gene therapy: role of gap-junctional intercellular communication. Cancer Res., *60:* 3989–3999, 2000.

Available online at www.sciencedirect.com
SCIENCE DIRECT®
Biochemical and Biophysical Research Communications 318 (2004) 935–940
BBRC
www.elsevier.com/locate/ybbrc

Aire downregulates multiple molecules that have contradicting immune-enhancing and immune-suppressive functions

Kojiro Sato,[a,*,1] Utako Sato,[b,1] Shoko Tateishi,[a] Kanae Kubo,[a] Reiko Horikawa,[b] Toshihide Mimura,[c] Kazuhiko Yamamoto,[a] and Hiroko Kanda[a]

[a] *Department of Allergy and Rheumatology, Graduate School of Medicine and Faculty of Medicine, University of Tokyo, Hongo 7-3-1, Bunkyo-ku, Tokyo 113-8655, Japan*
[b] *Division of Endocrinology and Metabolism, Department of Medicine, National Center for Child Health and Development, Okura 2-10-1, Setagaya-ku, Tokyo 157-8535, Japan*
[c] *Division of Rheumatology and Applied Immunology, Department of Medicine, Saitama Medical School, Morohongo 38, Moro-cho, Iruma-gun, Saitama 350-0495, Japan*

Received 14 April 2004
Available online 7 May 2004

Abstract

Autoimmune polyendocrinopathy-candidiasis-ectodermal dystrophy (APECED) is a systemic disease with autoimmune characteristics caused by mutations in a single gene called *AIRE*. Although a defect in negative selection has been emphasized for the pathogenesis of the autoimmune symptoms on the basis of studies of *Aire*-targeted mice, the function of the gene in the peripheral immune system and the cause of immunodeficiency noted in the disease have not been clarified yet. In this study, we demonstrated using murine *Aire* transfectants that Aire downregulates IL-1 receptor antagonist (IL-1Ra), which is important for immune suppression, and major histocompatibility complex (MHC) class II molecules, which are critical for acquired immunity. It was surprising to learn that Aire, which has been supposed to positively regulate transcription, downregulates multiple molecules. This downregulation of IL-1Ra and MHC class II molecules seems to be caused by the competition for transcriptional coactivator, CREB-binding protein (CBP), and may explain part of the contradictory (i.e., both autoimmune and immunodeficient) nature of APECED.

Keywords: AIRE; APECED; IL-1 receptor antagonist; MHC class II molecule; CREB-binding protein

Autoimmune polyendocrinopathy-candidiasis-ectodermal dystrophy (APECED; OMIM 240300) or autoimmune polyglandular syndrome type I (APS I) is an autosomal recessive disease characterized by multiple organ damage probably caused by autoimmune mechanisms [1]. The damage mainly affects endocrine organs and results in pathological conditions, such as hypoparathyroidism, adrenocortical failure, diabetes mellitus, gonadal failure, pernicious anemia, hypothyroidism, and hepatitis. Concurrently, this disease has an immunodeficiency aspect, chronic mucocutaneous candidiasis.

This disease is caused by mutations of a single gene, called *AIRE* (autoimmune regulator), on chromosome 21 [2–4]. Finns, Sardinians, and Iranian Jews were reported to have a high prevalence of the disease [1,5,6]. The protein coded by this gene has a nuclear localization signal (NLS), an HSR dimerization domain, a SAND domain, four LXXLL motifs, two PHD-type zinc-finger motifs, and a proline-rich region, suggesting that the protein can function as a transcription factor [7,8]. Indeed, AIRE exhibits a transcriptional activity [9,10].

The expression of AIRE is restricted to certain limited cells, such as thymic medullary epithelial cells, peripheral macrophages, and dendritic cells [11,12]. Recently, the failure to delete some organ-specific T cells in the thymus (negative selection) has been claimed to be

* Corresponding author. Fax: +81-3-5449-5433.
E-mail addresses: satok.cell@tmd.ac.jp, satok-tky@umin.ac.jp (K. Sato), .
[1] These authors contributed equally to the work.

0006-291X/$ - see front matter © 2004 Elsevier Inc. All rights reserved.
doi:10.1016/j.bbrc.2004.04.116

the main cause of the disease ([13,14], see Discussion). However, the target genes of AIRE in the peripheral immune system and the mechanism(s) of immunodeficiency are almost unknown. In this study, we analyzed the target genes of murine Aire using stable transfectants and investigated the mechanisms underlying the disease.

Materials and methods

Cells and reagents. Raw 264.7 cells were kindly provided by Dr. Hiroshi Takayanagi. Lipopolysaccharide (LPS) from *Escherichia coli* serotype 055:B5 was purchased from Sigma. Recombinant mouse interferon-γ (IFN-γ) was purchased from Genzyme/Techne. FITC-labeled mAb against MHC class II molecule (AMS-32.1) was purchased from BD PharMingen. Polyclonal Ab against murine CBP (A-22) was purchased from Santa Cruz Biotechnology. CBP-expressing vector was kindly provided by Dr. Akiyoshi Fukamizu [15].

Production of stable transfectants. Mouse Aire cDNA was obtained by RT-PCR using total RNA from the mouse spleen. The primers used were as follows.

Sense: 5′-TCTAGACAGCCCCTGTGAGGAAGATGGCAGGT GGGG-3′

Antisense: 5′-TCTAGAGTCATCAGGAAGAGAAGGGTGGT GTCTCGG-3′ (mouse *Aire* gene, Accession No. AJ243821)

The subcloned genes were sequenced and one clone with no mutation was selected. It was excised from its host plasmid by *Xba*I restriction and was religated into the *Xba*I site of the pBK-CMV phagemid vector (Stratagene). A mutant Aire-expressing vector (Aire(1–293)) was constructed from this vector by PCR [16] using the following primers.

Sense: 5′-TGATGACTCTAGAGCGGCCG-3′

Antisense: 5′-AACCTGGGGCTCACTGGGGA-3′

Raw 264.7 cells were transfected with the Aire-expressing vector and control empty vector using FuGENE 6 (Roche) according to the manufacturer's instructions. Stable transfectants were selected using G418 (500 μg/ml, Invitrogen) for 2 weeks until individual colonies were formed on the plate. They were used either as clones or in bulk.

Ribonuclease protection assay. RiboQuant RNase Protection Assay Systems (BD Biosciences) were used according to the manufacturer's instructions. The mouse cytokine/chemokine sets, mCK-2b and mCK-5, were used.

Luciferase assay. Genomic DNA corresponding to the 5′ upstream region of the mouse *IL-1Ra* gene (Accession Nos. L32838 and AL732528) was cloned by RT-PCR, using the primers listed below.

Sense (1): 5′-GAGCTCCACTTTTCCATGATTTGGG-3′

Sense (2): 5′-GAGCTCTAGGGCAGAGGTCAGCA-3′

Sense (3): 5′-GAGCTCGGGACAGGGGGATCAGCA-3′

Sense (4): 5′-GAGCTCTCTGACAGTGGAACGGAATG-3′

Antisense: 5′-AAGCTTCCGAGGCCACAGCAAGGCAA-3′

The four sequences were excised from its host plasmid by *Hin*dIII and *Sac*I restriction sites and were religated into the gap between the *Hin*dIII and *Sac*I sites of the Picagene luciferase reporter plasmid (Wako Pure Chemical). A mutant reporter construct was generated in the same way as the mutant Aire(1–293) vector. The used primers were as follows.

Sense: 5′-ATAGGCTCTTGTCTGCAAACATAACAGAGTATC ATTAATGTTTTCAGGGA-3′

Antisense: 5′-TGTGGTCCTCTGTGAAGTTGGAGTCCTTTAG AGGTGTTTTCATTCCC-3′

Transient transfection and luciferase assays were performed basically as described previously [17]. Briefly, cells were seeded into a 48-well plate (2×10^5 cells/well) and transfected with the reporter plasmid at 0.5 μg/well. After 36 h, 100 ng/ml LPS was added to the medium and 12 h later, the cells were harvested and luciferase activity was measured. An empty pBK-CMV vector was used to adjust the transfected DNA quantity. An empty luciferase reporter plasmid was used as control to calculate relative luciferase unit.

Chromatin immunoprecipitation. The Aire transfectants or control cells (2×10^6/well) were cultured with or without 100 ng/ml LPS for 6 h. After that, cells were harvested and processed using a Chromatin Immunoprecipitation Assay kit (Upstate Biotechnology) according to the manufacturer's instructions. The primers used for PCR were sense (1) described above and the antisense primer 5′-TGCTGACCTCT GCCCTAGAG-3′ (complementary sequence of sense (2)).

Flow cytometric analysis. Stable transfectants and control cells were stimulated with 100 U/ml IFN-γ for 24 h. After that, the cells were harvested and nonspecific staining was blocked with anti-CD16/CD32 mAb (Fc block, 2.4G2). The cells were then incubated with Class II Ab for 20 min, after which they were washed twice with PBS containing 0.5% bovine serum albumin. The cells were analyzed on a FACSCalibur using CellQuest software (Beckton–Dickinson). Viable cells were gated on the basis of forward and side scatters and by propidium iodide staining.

Results

First, we established two lines of the murine Aire transfectant from macrophage-lineage Raw 264.7 cells. Two control lines were also established into which an empty vector was introduced. Aire mRNA expression was confirmed by Northern blotting (Fig. 1). We obtained total RNA from these cells with or without lipopolysaccharide (LPS) stimulation and analyzed the mRNA expression levels of cytokines and chemokines by a ribonuclease protection assay (Fig. 2A). Neither cytokine nor chemokine was induced more in the Aire-expressing cells than in the control cells. This was surprising because Aire has been considered to be a positive transcription factor [9,10]. On the contrary, IL-1 receptor antagonist (IL-1Ra) mRNA level was significantly decreased in the Aire-expressing cells compared with the control cells after LPS stimulation. The expression levels of other cytokines, such as macrophage migration inhibitory factor (MIF), and chemokines we investigated exhibited little difference between the Aire-expressing cells and the control cells (Fig. 2B).

Next, we sought in silico the 5′ flanking region of the murine *IL-1Ra* gene that was most affected by Aire expression (Fig. 3A) and noted a NF-κB-binding sequence

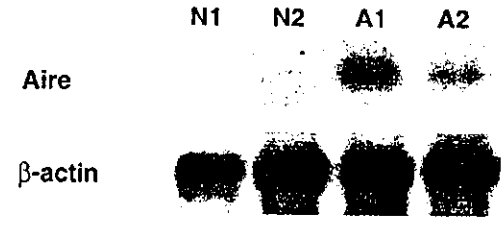

Fig. 1. Expression levels of Aire and β-actin mRNA. Five micrograms each of total RNA obtained from two Aire transfectants (clones A1 and A2) and two control cells (clones N1 and N2) was analyzed by Northern blotting. No intrinsic Aire mRNA was detected in the control cells.

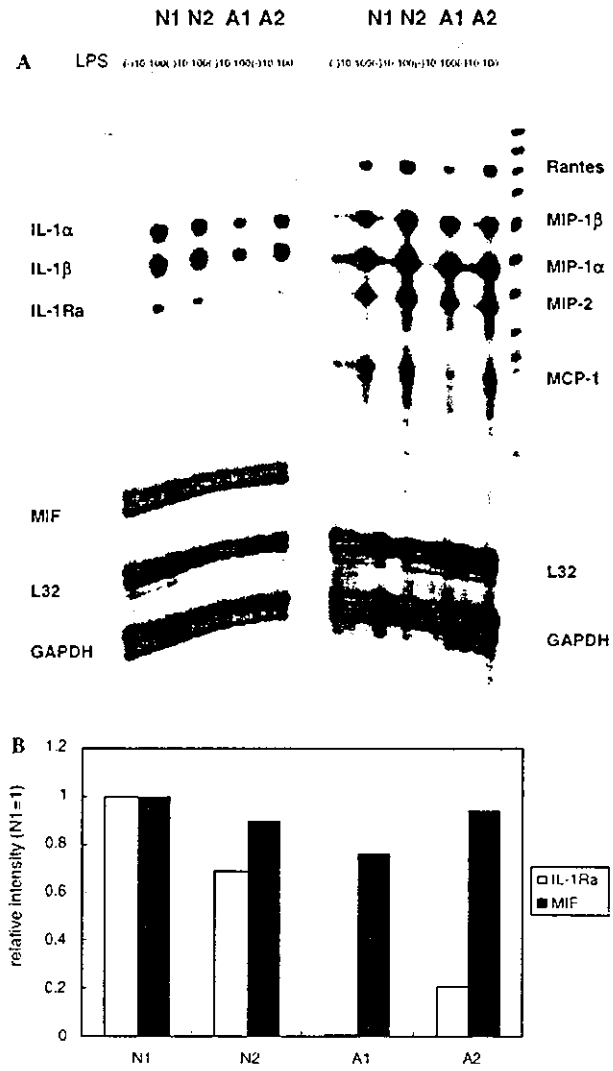

Fig. 2. Ribonuclease protection assay of cytokine and chemokine mRNA expressed by Aire transfectants and control cells. (A) Three micrograms each of total RNA obtained from these cells with or without 8-h LPS stimulation (10 or 100 ng/ml) was analyzed. The analyzed cytokines and chemokines were: IL-12p35, IL-10, IL-1α, IL-1β, IL-1Ra, IL-18, IL-6, IFN-γ, and MIF (left side) and Ltn, RANTES, Eotaxin, MIP-1β, MIP-1α, MIP-2, IP-10, MCP-1, and TCA-3 (right side). L32 and GAPDH were used as controls. The lanes on the extreme left and right represent probe-only (i.e., without RNA) control lanes. (B) Quantification of expression levels of IL-1Ra and MIF. The intensity of the blots of the above data was quantified and standardized using clone N1 as 1. Data shown are representative of three independent experiments. Hereafter, clones A1 and N1 were used as the Aire-expressing cells and control cells, respectively, if not mentioned otherwise.

and an interferon-stimulated response element (ISRE), to which interferon regulatory factor (IRF) family transcriptional factors bind [18], near the translation initiation site. This region probably has a capacity to respond to inflammatory stimulation. At about 1000 bp upstream of this region, two cyclic AMP response elements (CREs) appeared in tandem, which are supposed to be bound by CRE-binding proteins (CREBs). Considering the observation that AIRE can bind to a CREB-binding protein (CBP) [10], which can be recruited to CRE via CREB, Aire overexpression may affect this region and cause IL-1Ra downregulation.

Therefore, we generated a luciferase reporter construct that contained the region including two CREs, ISRE, and NF-κB-binding sequence (construct A) and also three shorter constructs (B–D). The shortest one (D) contained no CREs, ISRE nor NF-κB-binding sequence (Fig. 3B). We transiently transfected these vectors into the Aire-expressing cells and control cells, then stimulated them with LPS and analyzed luciferase activity. As expected, construct D did not respond to LPS stimulation irrespective of Aire expression. On the other hand, the longest construct (A) exhibited less luciferase activity induction after LPS stimulation in the Aire-expressing cells than in the control cells. The other two constructs exhibited similar response to LPS stimulation in both cells (Fig. 3C). The fact that construct A exhibited less luciferase activity than construct B in Aire-expressing cells irrespective of LPS stimulation indicates that construct A contains negative element(s), which becomes apparent in the presence of Aire. These results also suggest that Aire expression reduces IL-1Ra promoter responsiveness to LPS stimulation through a CRE-related mechanism. To confirm this, we constructed a mutant-Aire expression vector (Aire(1–293)), which lacks a proline-rich region and both of the PHD-type zinc finger domains and has no transcriptional transactivation property [10], and a mutant luciferase reporter gene which has mutations in both of the CREs and did similar experiment, this time not using clones but using transfectants in bulk. LPS stimulation did not exhibit an Aire-mediated repression of luciferase activity when Raw cells were transfected with Aire(1–293) (Fig. 4A). Moreover, when the mutant luciferase reporter construct was used, very little luciferase activity was detected either with wild type Aire or mutant Aire. These results strongly favor the hypothesis of CRE-dependent luciferase downregulation by Aire. Then what is the underlying mechanism of the downregulation? CBP competition may be one possibility. That is, the binding of Aire to CBP leads to the lack of this transcriptional coactivator binding to the IL-1Ra promoter, thus causing a decrease in the extent of IL-1Ra induction.

To assess whether the lack of CBP causes this reporter's unresponsiveness to LPS, we attempted to rescue the luciferase induction using a CBP expression vector. As expected, CBP overexpression rescued the responsiveness to LPS in a dose-dependent manner (Fig. 4B). On the other hand, when mutant Aire was introduced into the cells, the responsiveness to LPS was not affected by the overexpression of CBP, further indicating that the lack of CBP is indeed the cause of the

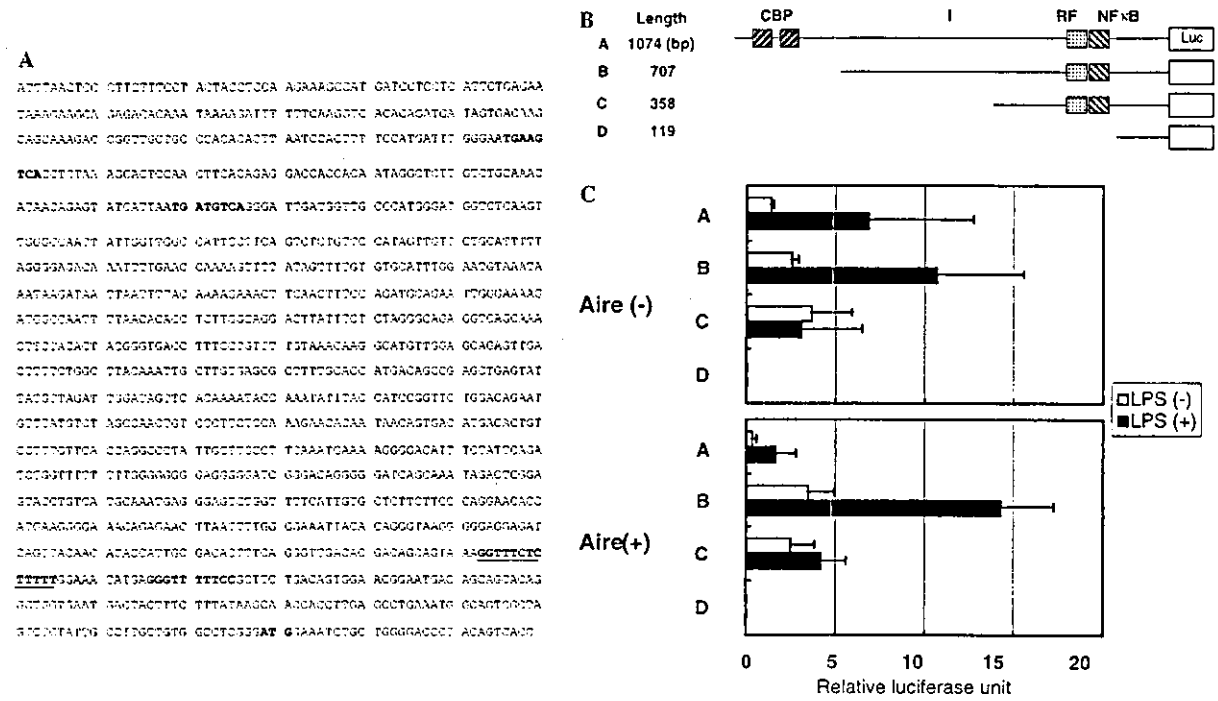

Fig. 3. Promoter analysis of IL-1Ra. (A) 5′-flanking region of the murine IL-1Ra gene (Accession Nos. L32838 and AL732528). Double underlines indicate CRE, to which the CRE-binding protein binds. A single underline indicates ISRE, to which IRF family transcription factors bind and the dotted underline indicates the site to which NF-κB binds. The bold ATG indicates the translation initiation site. (B) Four constructions of IL-1Ra-Luc reporter. (C) IL-1Ra-Luc reporter assay in Aire transfectants and control cells. These cells were transfected with each of the reporters with or without 12-h LPS stimulation (100 ng/ml) prior to the estimation of luciferase activity.

reporter construct's unresponsiveness to LPS. To clarify whether CBP is actually recruited to the IL-1Ra promoter, we performed chromatin immunoprecipitation (ChIP) assay using an anti-CBP antibody. As shown in Fig. 4C, the IL-1Ra-specific sequence was amplified only in the immunoprecipitated sample from LPS-stimulated control cells. This indicates that after LPS stimulation, the transcriptional complex containing CBP is recruited to the IL-1Ra promoter. On the other hand, no band was detected from the Aire-expressing cells irrespective of LPS stimulation, indicating that Aire expression inhibits the recruitment of CBP to this promoter. A similar mechanism has been proposed in the induction of MHC class II expression [19]. Two factors, CIITA and CBP, are necessary for the induction of this molecule [20]. It is postulated that glucocorticoid treatment leads to a reduction in class II molecule expression level due to the squelching of CBP by the glucocorticoid receptor. Thus, it is expected that the class II molecule expression is also downregulated by Aire in the same manner as in the presence of glucocorticoid. This was indeed the case. Raw 264.7 cells express class II molecules after IFN-γ treatment [21]. Although both Aire-expressing cells and control cells showed a low class II molecule expression level on the cell surface without IFN-γ stimulation, the former cells showed a much lower expression level of class II molecules than the latter cells after IFN-γ stimulation (Fig. 5).

Discussion

Aire has been supposed to be a transcription factor [7–10]. Recently, the gene chip analysis of Aire-knock-out mice has revealed that the transcription of peripheral organ-specific genes is reduced in *Aire*-deficient thymic medullary epithelial cells [13]. The authors of the above paper and others claimed that the failure to delete some organ-specific T cells in the thymus (failure of negative selection) is the main cause of the inflammation of multiple organs in the Aire-knock-out mice (and probably in APECED patients) [13,14]. However, this theory does not explain all aspects of APECED. For example, it does not explain the function of Aire expressed in the periphery, such as in macrophages and dendritic cells. Immunodeficiency observed in APECED patients cannot be explained by this mechanism, either. The fact that both APECED patients and Aire-knock-out mice show significant phenotypic variability indicates that external factors, such as infection, may play important roles in the pathogenesis of the disease [22].

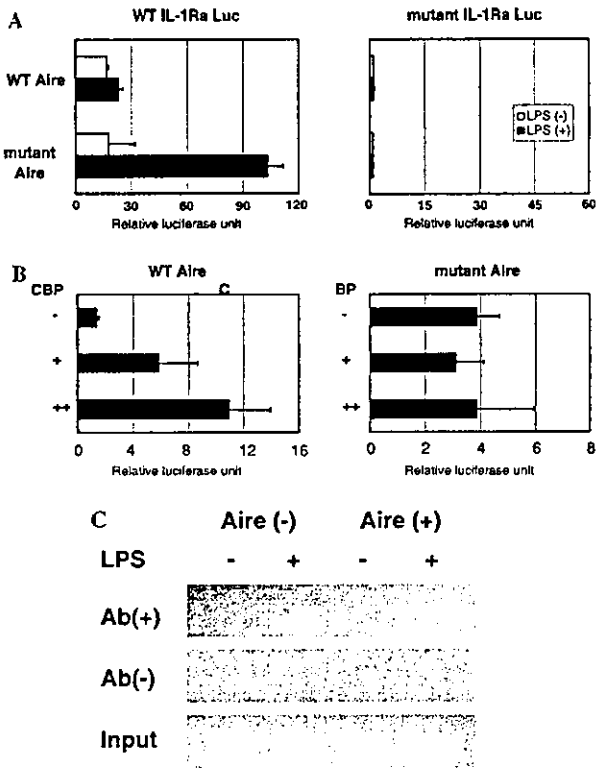

Fig. 4. Aire-mediated dampened response of the IL-1Ra promoter to LPS was dependent on CREs and rescued by CBP. (A) Mutant Aire showed little effect of dampening the IL-1Ra promoter responsiveness to LPS stimulation. The mutant IL-1Ra promoter that lacked two CREs showed little promoter activity in response to LPS irrespective of the cotransfection of wild-type or mutant Aire. (B) The cotransfection of CBP rescued the responsiveness of the IL-1Ra promoter to LPS in a dose-dependent manner (CBP+: 0.625 μg expression vector/well, ++: 1.25 μg expression vector/well). In the case of mutant Aire, CBP cotransfection did not affect the responsiveness of the IL-1Ra promoter. (C) The anti-CBP antibody could immunoprecipitate the IL-1Ra promoter region of the control cells after LPS stimulation. No band for the region was detected by PCR in the absence of the antibody. In the case of the Aire-expressing cells, the region was not immunoprecipitated even after LPS stimulation.

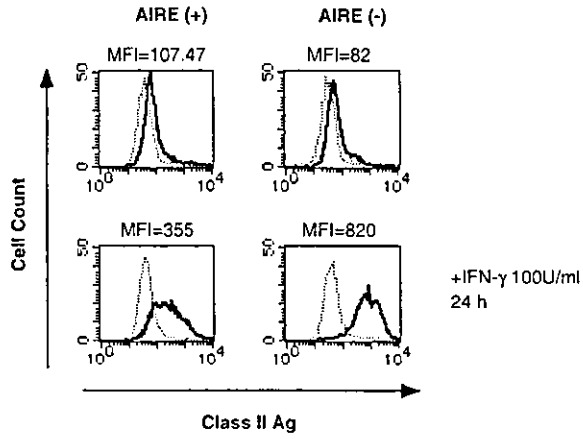

Fig. 5. Induction of class II molecule expression on Aire transfectant and control cells by IFN-γ. These cells were cultured with or without 24-h IFN-γ stimulation (100 U/ml) prior to flow cytometric analysis. Dotted lines represent background staining with control rat IgG. MFI, mean fluorescence intensity.

In this report, we have observed that Aire can negatively regulate multiple genes, contrary to previous reports arguing that Aire is a positive transcription factor [9,10]. Considering that IL-1Ra is supposed to prevent immunological responses by competitively inhibiting the biological effects of IL-1 [23,24] and that MHC class II molecules are critical for adaptive immune responses, the inhibition of the induction of both IL-1Ra and MHC class II molecules by Aire may explain the dual aspects of APECED, i.e., autoimmunity and immunodeficiency. This finding is even more interesting because IL-1 has been considered to be one of the important cytokines in the defense against *Candida albicans* infection [25], and candidiasis is among many traits of APECED [1]. Therefore, it would be of interest to investigate the expression level of these genes in APECED patients and two Aire-targeted mice lines [13,22].

As for the mechanisms underlying Aire-mediated downregulation of the above-mentioned molecules, the promoter assay showed that dampened response to LPS by Aire is dependent on the two CREs in the IL-1Ra promoter (Fig. 4A) and that CBP overexpression rescues the responsiveness (Fig. 4B). Moreover, the ChIP assay showed that Aire expression inhibits the recruitment of CBP to the IL-1Ra promoter containing the two CREs (Fig. 4C). This suggests that the squelching of the transcriptional coactivator by Aire may explain the downregulation of IL-1Ra. MHC class II molecules are downregulated by the squelching of CBP [19] and, as expected, they are also downregulated in the Aire-expressing cells (Fig. 5). We are now screening the genes that are differentially expressed depending on the existence of Aire, using the exhaustive cloning method of suppression subtractive hybridization (SSH). It seems that more genes are positively regulated than negatively regulated by Aire (data not shown). We are now identifying the genes to investigate whether some of the differentially regulated genes further explain the mechanisms underlying the downregulation of the gene expression described in this paper and the pathogenesis of APECED.

Acknowledgment

We gratefully acknowledge Dr. Shin-Ichiro Takahashi for thoughtful discussion.

References

[1] P. Ahonen, Autoimmune polyendocrinopathy-candidosis-ectodermal dystrophy (APECED): autosomal recessive inheritance, Clin. Genet. 27 (1985) 535–542.

[2] J. Aaltonen, P. Bjorses, L. Sandkuijl, J. Perheentupa, L. Peltonen, An autosomal locus causing autoimmune disease: autoimmune polyglandular disease type I assigned to chromosome 21, Nat. Genet. 8 (1994) 83–87.
[3] K. Nagamine, P. Peterson, H.S. Scott, J. Kudoh, S. Minoshima, M. Heino, K.J. Krohn, M.D. Lalioti, P.E. Mullis, S.E. Antonarakis, K. Kawasaki, S. Asakawa, F. Ito, N. Shimizu, Positional cloning of the APECED gene, Nat. Genet. 17 (1997) 393–398.
[4] The Finnish-German APECED Consortium – Group 1: Johanna Aaltonen, Petra Bjorses, Jaakko Perheentupa, Nina Horelli-Kuitunen, Aarno Palotie, Leena Peltonen; Group 2: Yeon Su Lee, Fiona Francis, Steffen Hennig, Cora Thiel, Hans Lehrach, Marie-Laure Yaspo. An autoimmune disease, APECED, caused by mutations in a novel gene featuring two PHD-type zinc-finger domains. The Finnish-German APECED consortium. Autoimmune polyendocrinopathy-candidiasis-ectodermal dystrophy, Nat. Genet. 17 (1997) 399–403.
[5] M.C. Rosatelli, A. Meloni, M. Devoto, A. Cao, H.S. Scott, P. Peterson, M. Heino, K.J. Krohn, K. Nagamine, J. Kudoh, N. Shimizu, S.E. Antonarakis, A common mutation in Sardinian autoimmune polyendocrinopathy-candidiasis-ectodermal dystrophy patients, Hum. Genet. 103 (1998) 428–434.
[6] J. Zlotogora, M.S. Shapiro, Polyglandular autoimmune syndrome type I among iranian jews, J. Med. Genet. 29 (1992) 824–826.
[7] T.J. Gibson, C. Ramu, C. Gemund, R. Aasland, The APECED polyglandular autoimmune syndrome protein, AIRE-1, contains the SAND domain and is probably a transcription factor, Trends Biochem. Sci. 23 (1998) 242–244.
[8] C. Rinderle, H.M. Christensen, S. Schweiger, H. Lehrach, M.L. Yaspo, AIRE encodes a nuclear protein co-localizing with cytoskeletal filaments: altered sub-cellular distribution of mutants lacking the PHD zinc fingers, Hum. Mol. Genet. 8 (1999) 277–290.
[9] P. Bjorses, M. Halonen, J.J. Palvimo, M. Kolmer, J. Aaltonen, P. Ellonen, J. Perheentupa, I. Ulmanen, L. Peltonen, Mutations in the AIRE gene: effects on subcellular location and transactivation function of the autoimmune polyendocrinopathy-candidiasis-ectodermal dystrophy protein, Am. J. Hum. Genet. 66 (2000) 378–392.
[10] J. Pitkanen, V. Doucas, T. Sternsdorf, T. Nakajima, S. Aratani, K. Jensen, H. Will, P. Vahamurto, J. Ollila, M. Vihinen, H.S. Scott, S.E. Antonarakis, J. Kudoh, N. Shimizu, K. Krohn, P. Peterson, The autoimmune regulator protein has transcriptional transactivating properties and interacts with the common coactivator CREB-binding protein, J. Biol. Chem. 275 (2000) 16802–16809.
[11] S. Zuklys, G. Balciunaite, A. Agarwal, E. Fasler-Kan, E. Palmer, G.A. Hollander, Normal thymic architecture and negative selection are associated with Aire expression, the gene defective in the autoimmune-polyendocrinopathy-candidiasis-ectodermal dystrophy (APECED), J. Immunol. 165 (2000) 1976–1983.
[12] K. Kogawa, S. Nagafuchi, H. Katsuta, J. Kudoh, S. Tamiya, Y. Sakai, N. Shimizu, M. Harada, Expression of AIRE gene in peripheral monocyte/dendritic cell lineage, Immunol. Lett. 80 (2002) 195–198.
[13] M.S. Anderson, E.S. Venanzi, L. Klein, Z. Chen, S.P. Berzins, S.J. Turley, H. von Boehmer, R. Bronson, A. Dierich, C. Benoist, D. Mathis, Projection of an immunological self shadow within the thymus by the aire protein, Science 298 (2002) 1395–1401.
[14] A. Liston, S. Lesage, J. Wilson, L. Peltonen, C.C. Goodnow, Aire regulates negative selection of organ-specific T cells, Nat. Immunol. 4 (2003) 350–354.
[15] E. Yoshida, T. Nakajima, K. Murakami, A. Fukamizu, Identification of N-terminal minimal transactivation domain of CBP, p300 and *Caenorhabditis elegans* homologues, Gene 208 (1998) 307–314.
[16] Y. Imai, Y. Matsushima, T. Sugimura, M. Terada, A simple and rapid method for generating a deletion by PCR, Nucleic Acids Res. 19 (1991) 2785.
[17] K. Sato, S. Hida, H. Takayanagi, T. Yokochi, N. Kayagaki, K. Takeda, H. Yagita, K. Okumura, N. Tanaka, T. Taniguchi, K. Ogasawara, Antiviral response by natural killer cells through TRAIL gene induction by IFN-alpha/beta, Eur. J. Immunol. 31 (2001) 3138–3146.
[18] T. Taniguchi, K. Ogasawara, A. Takaoka, N. Tanaka, IRF family of transcription factors as regulators of host defense, Annu. Rev. Immunol. 19 (2001) 623–655.
[19] J.D. Fontes, S. Kanazawa, D. Jean, B.M. Peterlin, Interactions between the class II transactivator and CREB binding protein increase transcription of major histocompatibility complex class II genes, Mol. Cell. Biol. 19 (1999) 941–947.
[20] A. Kretsovali, T. Agalioti, C. Spilianakis, E. Tzortzakaki, M. Merika, J. Papamatheakis, Involvement of CREB binding protein in expression of major histocompatibility complex class II genes via interaction with the class II transactivator, Mol. Cell. Biol. 18 (1998) 6777–6783.
[21] T.A. Wynn, Y.R. Freund, D.M. Paulnock, TNF-alpha differentially regulates Ia antigen expression and macrophage tumoricidal activity in two murine macrophage cell lines, Cell Immunol. 140 (1992) 184–196.
[22] C. Ramsey, O. Winqvist, L. Puhakka, M. Halonen, A. Moro, O. Kampe, P. Eskelin, M. Pelto-Huikko, L. Peltonen, Aire deficient mice develop multiple features of APECED phenotype and show altered immune response, Hum. Mol. Genet. 11 (2002) 397–409.
[23] D.J. Dripps, B.J. Brandhuber, R.C. Thompson, S.P. Eisenberg, Interleukin-1 (IL-1) receptor antagonist binds to the 80-kDa IL-1 receptor but does not initiate IL-1 signal transduction, J. Biol. Chem. 266 (1991) 10331–10336.
[24] E.V. Granowitz, B.D. Clark, J. Mancilla, C.A. Dinarello, Interleukin-1 receptor antagonist competitively inhibits the binding of interleukin-1 to the type II interleukin-1 receptor, J. Biol. Chem. 266 (1991) 14147–14150.
[25] J.W. Van't Wout, J.W. Van der Meer, M. Barza, C.A. Dinarello, Protection of neutropenic mice from lethal *Candida albicans* infection by recombinant interleukin 1, Eur. J. Immunol. 18 (1988) 1143–1146.

Transendothelial Migration of Human Basophils[1]

Motoyasu Iikura,[2]* Motohiro Ebisawa,[‡] Masao Yamaguchi,* Hiroshi Tachimoto,[‡] Ken Ohta,[§] Kazuhiko Yamamoto,* and Koichi Hirai[†]

During allergic reactions, basophils migrate from the blood compartment to inflammatory sites, where they act as effector cells in concert with eosinophils. Because transendothelial migration (TEM) represents an essential step for extravasation of cells, for the first time we have studied basophil TEM using HUVEC. Treatment of HUVEC with IL-1β significantly enhanced basophil TEM, which was further potentiated by the presence of a CCR3-specific ligand, eotaxin/CCL11. In addition to CCR3 ligands, MCP-1/CCL2 was also active on basophil TEM. Although stromal cell-derived factor-1/CXCL12, a CXCR4 ligand, failed to induce TEM in freshly isolated basophils, it caused strong TEM in 24-h cultured cells. IL-3 enhanced basophil TEM by increasing the chemokinetic response. Spontaneous TEM across activated HUVEC was inhibited by treatment of cells with anti-CD18 mAb, but not with anti-CD29 mAb, and also by treatment of HUVEC with anti-ICAM-1 mAb. Anti-VCAM-1 mAb alone failed to inhibit TEM, but showed an additive inhibitory effect in combination with anti-ICAM-1 mAb. In contrast, eotaxin- and IL-3-mediated TEM was significantly inhibited by anti-CD29 mAb as well as anti-CD18 mAb. These results indicate that β_2 integrins play the primary role in basophil TEM, but β_1 integrins are also involved, especially in TEM of cytokine/chemokine-stimulated basophils. In conclusion, the regulatory profile of basophil TEM is very similar to that reported for eosinophils. Our results thus support the previous argument for a close relationship between basophils and eosinophils and suggest that the in vivo kinetics of these two cell types are similar. *The Journal of Immunology*, 2004, 173: 5189–5195.

Although basophils are the least abundant circulating leukocytes, an increasing body of evidence has demonstrated that these cells play an active pathogenic role in allergic inflammation by releasing diverse proinflammatory mediators, including vasoactive amines, cysteinyl leukotrienes, and cytokines (1). The biological significance of basophils in allergic disorders has become more apparent with the recognition and understanding of allergic dual-phase reactions; analyses of chemical mediators have revealed increases in basophil-derived mediators at the sites of late-phase reactions (2–4).

The results of experimental allergen challenge in various organs have revealed the influx of basophils to inflammatory sites several hours after Ag exposure (5–9), indicating the existence of a mechanism for recruitment of basophils from the blood compartment to inflamed tissue sites during allergic reactions. Like other types of leukocytes, the entire process of basophil influx to inflamed tissue sites comprises three essential sequential steps: adhesion to the vascular endothelium, transendothelial migration (TEM),[3] and locomotion toward inflammatory sites in extravascular tissues. To date, a considerable number of studies have outlined the mechanisms of both the adhesion and locomotion processes in basophils (10–14), demonstrating that adhesion molecules and/or several cytokines and chemokines are critically involved in these processes. In contrast to neutrophils, basophils express $\alpha_4\beta_1$ integrins in addition to β_2 integrins. Basophil-activating cytokines such as IL-3 are capable of up-regulating the expression of β_2 integrins (CD11b and CD18), thereby potentiating the β_2 integrin-mediated adherence of basophils to the endothelium (14). These basophil-activating cytokines also enhance basophil locomotive responses by inducing random movement (chemokinesis) (11). Regarding the basophil migration process, however, basophil-directed chemokines such as eotaxin play more critical roles by virtue of inducing strong directional movement (chemotaxis) (15, 16).

The molecular aspects of both the adhesion and migration processes of basophils have thus become increasingly clear, but those of basophil TEM, another essential process that links the adhesion process and the locomotion process, have not been studied to date. Given the importance of the TEM process for the recruitment of basophils to allergic inflammatory sites, for the first time we have studied basophil TEM using vascular endothelial cell monolayers.

Materials and Methods

Reagents and mAbs

Murine mAbs with blocking activity against adhesion molecules were used. Anti-CD49d mAb (IgG1, clone HP2/1) and anti-CD29 mAb (IgG1, clone 4B4) were purchased from Coulter Immunotech (Marseille, France). Anti-CD11a mAb (IgG1, clone TS1/22) was obtained from Endogen (Woburn, MA). Anti-CD49e mAb (IgG1, clone IIA1), anti-CD11b mAb (IgG1, clone 44), and anti-CD18 mAb (IgG1, clone L130) were purchased from BD Pharmingen (San Diego, CA). The $F(ab')_2$ of anti-CD54 mAb (IgG2a, clone MEM-111) and anti-CD106 mAb (IgG1, clone 1G11B1) were purchased from Caltag Laboratories (Burlingame, CA). The $F(ab')_2$ of mouse IgG was obtained from Jackson ImmunoResearch Laboratories (West Grove, PA). Mouse IgG1 (MOPC-21) with irrelevant specificity was purchased from Sigma-Aldrich (St. Louis, MO). Murine anti-CCR1 mAb (IgG1, clone 141) and anti-CCR3 mAb (IgG1, clone 444) were donated by Dr. H. Kawasaki (Institute of Medical Science, University of Tokyo, Tokyo, Japan) (17). Other reagents used in the experiments were previously described (13).

Departments of *Allergy and Rheumatology and [†]Bioregulatory Function, University of Tokyo Graduate School of Medicine, Tokyo, Japan; [‡]Department of Pediatrics, National Sagamihara Hospital, Kanagawa; and [§]Department of Medicine, Teikyo University School of Medicine, Tokyo, Japan

Received for publication December 23, 2003. Accepted for publication August 5, 2004.

The costs of publication of this article were defrayed in part by the payment of page charges. This article must therefore be hereby marked *advertisement* in accordance with 18 U.S.C. Section 1734 solely to indicate this fact.

[1] This work was supported by grants-in-aid from the Ministry of Health and Welfare of Japan and from the Ministry of Education, Science, Sports, and Culture of Japan.

[2] Address correspondence and reprint requests to Dr. Motoyasu Iikura, Department of Allergy and Rheumatology, University of Tokyo Graduate School of Medicine, 7-3-1 Hongo, Bunkyo-ku, Tokyo 113-8655, Japan. E-mail address: iikura-tky@umin.ac.jp

[3] Abbreviations used in this paper: TEM, transendothelial migration; MCP, monocyte chemoattractant protein; SDF, stromal cell-derived factor.

0022-1767/04/$02.00

Cell separation and culture conditions

Human basophils were isolated from venous blood obtained from consenting volunteers with no history of atopic diseases. Basophils were semipurified by Percoll density gradient centrifugation as previously described (18). The purity of semipurified basophil preparations was 12.5 ± 0.13% (n = 60). A vast majority of the contaminating cells were lymphocytes and monocytes, and the preparations usually contained no eosinophils. Their viability, measured by the trypan blue exclusion test, was consistently >95%. In some experiments basophils were further purified (purity, ~98%) by negative selection with MACS beads (Basophil Isolation kit; Miltenyi Biotec, Auburn, CA) as described previously (13).

HUVEC were isolated and cultured according to the previously described methods (19). The culture medium was medium 199 (Invitrogen Life Technologies, Grand Island, NY) supplemented with 20% FCS (Invitrogen Life Technologies), 2 mM L-glutamine (Invitrogen Life Technologies), antibiotics (100 U/ml penicillin and 100 μg/ml streptomycin; Invitrogen Life Technologies), endothelial cell growth supplement (20 μg/ml; Collaborative Research, Bedford, MA), and heparin sodium (90 μg/ml; Sigma-Aldrich). HUVEC (2–5 × 10^4 cells) were cultured on 2% gelatin-coated Transwell culture inserts (6.5-mm diameter polycarbonate membranes with 5-μm pores; Costar, Cambridge, MA) for 2–5 days. To confirm the confluence of the HUVEC on the membrane, sample monolayers were routinely stained with Diff-Quick (International Reagents, Kobe, Japan) before use in each experiment.

TEM assay

Unless otherwise indicated, HUVEC monolayers grown in Transwell inserts were pretreated for 4 h with human rIL-1β (5 ng/ml; Diaclone Research, Besaçn, France) and washed twice with PIPES ACM buffer (25 mM PIPES, 119 mM NaCl, 5 mM KCl, 2 mM Ca^{2+}, 0.5 mM Mg^{2+}, and 0.03% human serum albumin). Percoll-separated basophils (3 × 10^4/100 μl) suspended in PIPES ACM buffer were added to the upper wells, and samples to be tested (600 μl) were placed in the lower wells. After incubation for 3 h at 37°C, the cells that had migrated to the lower wells were collected and washed twice in PBS supplemented with 3% FCS and 0.1% NaN_3. For analysis of the numbers of migrated basophils, the cells were stained with FITC-conjugated goat anti-human IgE (BioSource International, Camarillo, CA) at 4°C for 30 min. After washing the cells, the numbers of FITC-positive cells were counted by flow cytometry as previously described (13). Basophil TEM was expressed as a percentage of the number of inoculated basophils.

The effects of integrins and CCRs were examined by treating cells with blocking mAbs or controls at 37°C for 30 min. Without washing, treated cells were placed in the upper wells. We used $F(ab')_2$ for blocking CD54 (ICAM-1) and CD106 (VCAM-1) on HUVEC to avoid the undesired effects of the Fc portion of immobilized mouse mAb on basophil FcγR. HUVEC were pretreated with the $F(ab')_2$ of each mAb or controls at 37°C for 30 min before assay. The inhibition by mAbs was calculated using the following formula: % inhibition = (migration by isotype-matched control-treated cells − migration by blocking mAb-treated cells)/(migration by isotype-matched control-treated cells) × 100.

Statistics

All data are expressed as the mean ± SEM, and differences between values were analyzed by the one-way ANOVA. When this test indicated a significant difference, Fisher's protected least significant difference test was used to compare individual groups.

Results

Effects of IL-1 and eotaxin on basophil migration across endothelial cells

A basophil TEM assay was performed using Percoll-separated basophils and Transwell systems with cultivated HUVEC on the surface. In accordance with the previous reports of eosinophil TEM assays (19), HUVEC were activated by stimulation with IL-1β for 4 h before assays. As shown in Fig. 1*A*, only marginal numbers of basophils had transmigrated across a layer of unstimulated HUVEC even after 3 h of incubation. In contrast, stimulation of HUVEC with IL-1β significantly enhanced basophil TEM at later time points. During the initial 2 h, TEM across IL-1-activated HUVEC showed a similar time course of accumulation as TEM across unstimulated HUVEC. After 3-h incubation, however, the

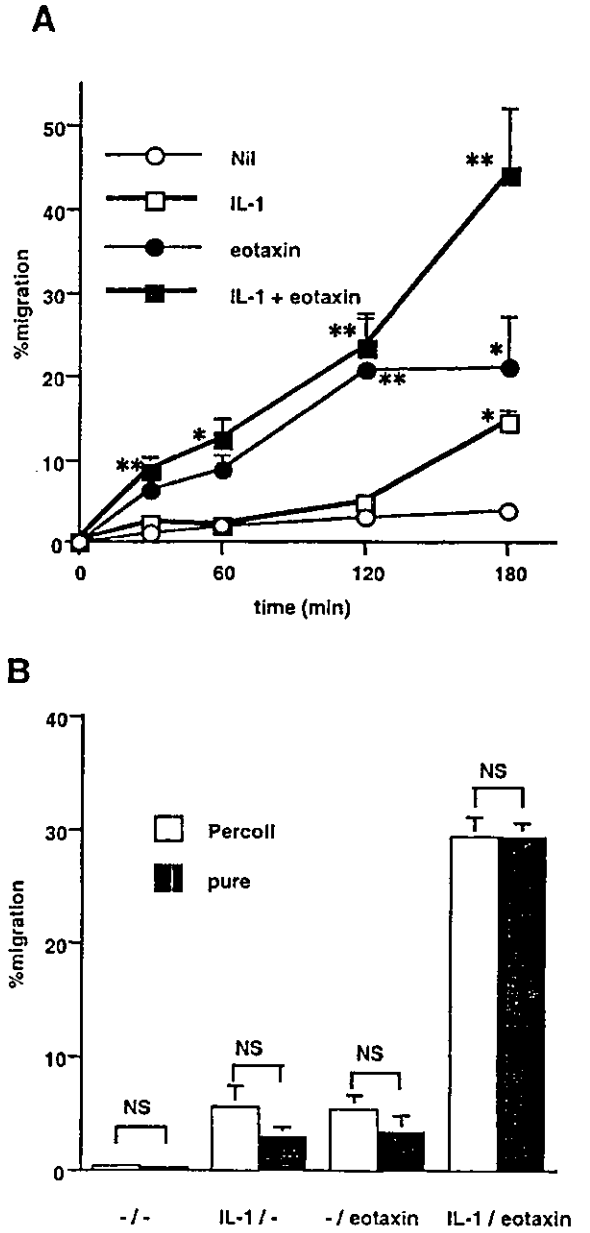

FIGURE 1. Time course of TEM of basophils. *A*, HUVEC monolayers in Transwell inserts were pretreated with (■ and □) and without (● and ○) IL-1-β (5 ng/ml) at 37°C for 4 h. Percoll-separated basophils were added to the upper wells, and the chambers were incubated at 37°C in the presence (■ and ●) and the absence (□ and ○) of eotaxin (5 nM) in the lower wells. After the indicated time periods, the cells in lower wells were collected, and the number of IgE-positive cells was determined by flow cytometry. Bars represent the SEM (n = 6–8). *, $p < 0.05$; **, $p < 0.01$ (vs spontaneous migration (○) at corresponding time point). *B*, TEM through HUVEC by highly purified basophils was indicated. Basophils from a sample of Percoll-separated cells were further enriched by negative selection with MACS beads. TEM assays were performed for 3 h, as described above, using Percoll- (□) and MACS-separated (■) basophils. The purities of Percoll- and MACS-separated basophils were 19.6 ± 5.7 and 98.3 ± 0.4%, respectively. Bars represent the SEM (n = 5). NS, no significant difference between Percoll- and MACS-separated basophils.

number of transmigrated cells was significantly increased in cultures stimulated with IL-1β (3.9 ± 1.2 and 14.7 ± 2.7%, for TEM across unstimulated and IL-1-stimulated HUVEC, respectively). Furthermore, basophil TEM was markedly enhanced by the presence of

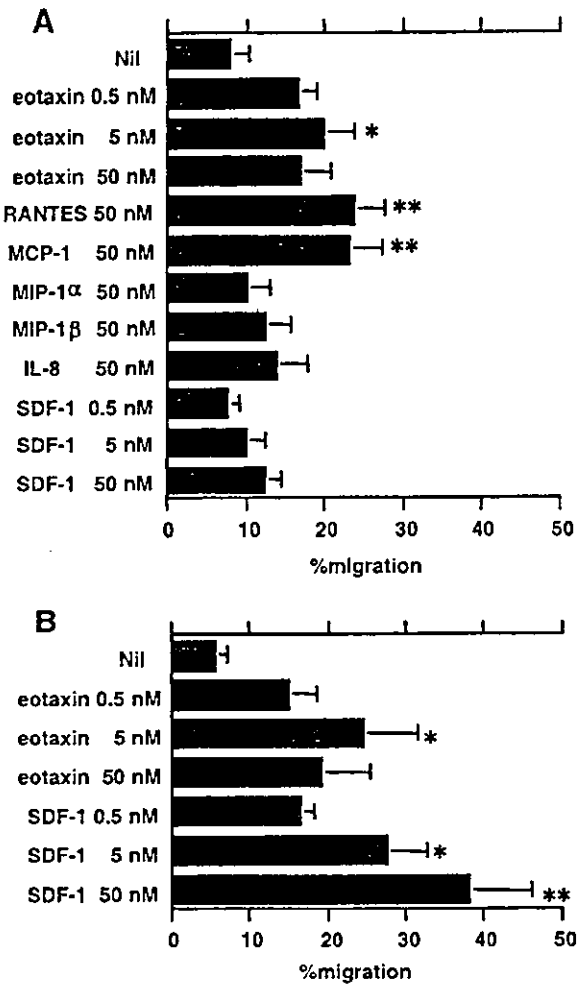

FIGURE 2. Effects of chemokines on basophil TEM. *A*, HUVEC were pretreated with IL-1-β (5 ng/ml) at 37°C for 4 h. A basophil TEM assay was performed in the presence of various chemokines in the lower wells. Basophils were separated by Percoll and immediately added to the upper wells. After 3 h of incubation at 37°C, the cells in the lower wells were collected, and the number of IgE-positive cells was determined by flow cytometry. *B*, Percoll-separated basophils were cultured in RPMI 1640 supplemented with 10% FCS and antibiotics at 37°C for 24 h. The cultured cells were added to the upper wells, and TEM assay was performed as described above. Bars represent the SEM (n = 4–7). *, $p < 0.05$; **, $p < 0.01$ (vs migration in the absence of chemokines (Nil)).

a chemoattractant, eotaxin/CCL11. Compared with spontaneous TEM, chemokine-induced TEM showed a faster time course of accumulation. Even with unstimulated HUVEC, the number of transmigrated cells increased linearly until 2 h and then plateaued. Although a similar time course of accumulation was observed with activated HUVEC until 2 h of incubation, the number of transmigrated cells was significantly increased at 3 h of incubation (Fig. 1*A*). The basophil preparations used in these experiments were Percoll-separated and consisted of ~90% contaminating cells. To explore whether these contaminating cells indirectly affect basophil TEM, we further purified the Percoll-separated cells by negative selection with MACS beads (purity, >98%) and compared the TEM between Percoll- and MACS-separated basophils. As shown in Fig. 1*B*, no significant difference in TEM was observed between the two preparations, indicating that contaminating cell populations do not significantly affect the basophil TEM.

Basophil TEM by chemokines

The results of our and other laboratories have demonstrated the expression of multiple chemokine receptors in basophils (13, 16, 20), and our previous functional survey demonstrated that CCR3 ligands are mainly responsible for the migratory responses of resting basophils (13). Fig. 2 depicts the effects of various chemokines on basophil TEM. Transmigration was determined after 3 h of incubation using IL-1-activated HUVEC. CCR3 ligands, eotaxin, and RANTES/CCL5 induced strong basophil TEM. Eotaxin binds specifically and exclusively to CCR3, whereas RANTES binds to CCR1 with higher affinity than to CCR3. To determine the chemokine receptors responsible for RANTES-induced basophil TEM, we performed blocking experiments using receptor-specific mAbs of an antagonistic nature. As shown in Fig. 3, eotaxin-induced TEM was almost completely inhibited by anti-CCR3 mAb. Although RANTES-induced TEM was also markedly blocked by anti-CCR3 mAb, treatment with anti-CCR1 mAb exerted virtually no effect on the migratory response.

Our previous study using a HUVEC-free Transwell system demonstrated that CXCR1/CXCR2 ligand IL-8/CXCL8 and CCR2 ligand MCP-1/CCL2 also induced significant, but weak, migration of basophils (13). However, no statistically significant TEM was observed in cells stimulated with IL-8. In contrast, MCP-1 was capable of inducing TEM as strongly as eotaxin. Furthermore, a CXCR4-specific ligand, stromal cell-derived factor-1 (SDF-1)/CXCL12, was also capable of inducing strong basophil TEM under certain conditions. In our previous report we demonstrated that the expression of functional CXCR4 is induced on the basophil surface by 24 h of culture, and SDF-1 induced significant migratory responses in 24-h cultured basophils (13). The same situation was observed in TEM; although freshly isolated basophils failed to exhibit TEM in response to SDF-1, strong TEM, comparable to that induced by eotaxin, was observed with 24-h cultured basophils (Fig. 2*B*).

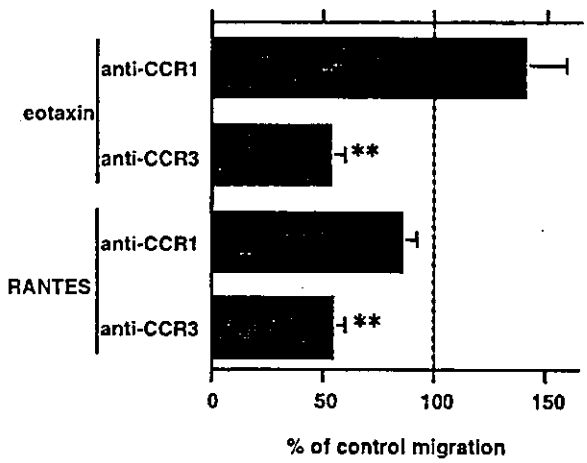

FIGURE 3. Effects of chemokine receptor blocking on chemokine-induced basophil TEM. HUVEC were pretreated with IL-1-β (5 ng/ml) at 37°C for 4 h. Percoll-separated basophils were preincubated with anti-chemokine receptor mAbs (20 μg/ml) or isotype control mAb (mouse IgG1, 20 μg/ml) at 37°C for 30 min. TEM assay was performed in the presence and the absence of eotaxin (15 nM) or RANTES (15 nM) in the lower wells for 3 h. Migrations of control Ab-treated basophils toward eotaxin and RANTES were 29.5 ± 4.6 and 28.5 ± 5.7%, respectively. Spontaneous migration without any chemokine was 9.2 ± 2.5%. Bars represent the SEM (n = 9). **, $p < 0.01$ (vs percentage of control migration).

Basophil TEM by IL-3

Results from our and other laboratories have established that IL-3 stimulates various aspects of basophil functions, such as mediator release (21, 22) and in vitro survival (23, 24). Furthermore, our earlier study using Boyden chamber systems demonstrated that IL-3 potently enhances in vitro locomotive responses by basophils (11). The migratory response induced by IL-3 was chemokinetic rather than chemotactic. When serially diluted IL-3 was added to the upper wells of a Transwell, we observed that the number of transmigrated basophils increased in a dose-dependent fashion (Fig. 4). A significant increase in basophil TEM was observed when the cell suspension in the upper wells contained as little as 3 pM IL-3. When the IL-3 gradient was diminished by adding the same concentration of IL-3 to both the upper and lower wells, the basophil TEM was not significantly affected. In contrast, elimination of the eotaxin gradient mostly inhibited the increase in basophil TEM, indicating that eotaxin-induced TEM was mainly chemotactic (Fig. 4). Furthermore, IL-3 showed an additive effect on eotaxin-induced TEM; the number of transmigrated cells induced by eotaxin was significantly increased in the presence of IL-3 (17.7 ± 4.4 and 23.4 ± 4.6%, eotaxin-induced TEM for the absence and the presence of IL-3, respectively; $n = 4$; $p < 0.05$).

Effects of adhesion molecules on basophil TEM

Adhesion molecules and their counter-receptors play a critical role in the TEM of various cell types. Previous studies by others revealed that basophils express both β_1 (CD49d, CD49e, and CD29) and β_2 (CD11a, CD11b, and CD18) integrins on their surface (25). When the effects of β_1 and β_2 integrins on basophil TEM across IL-1-stimulated HUVEC were studied using blocking mAbs, significant inhibition of spontaneous TEM was observed in cells treated with anti-CD18 mAb, but not in those treated with anti-CD29 mAb, in both Percoll-separated and MACS-separated basophils (Fig. 5*A*). No significant inhibition was observed in cells treated with anti-CD11a or anti-CD11b mAb alone, but treatment

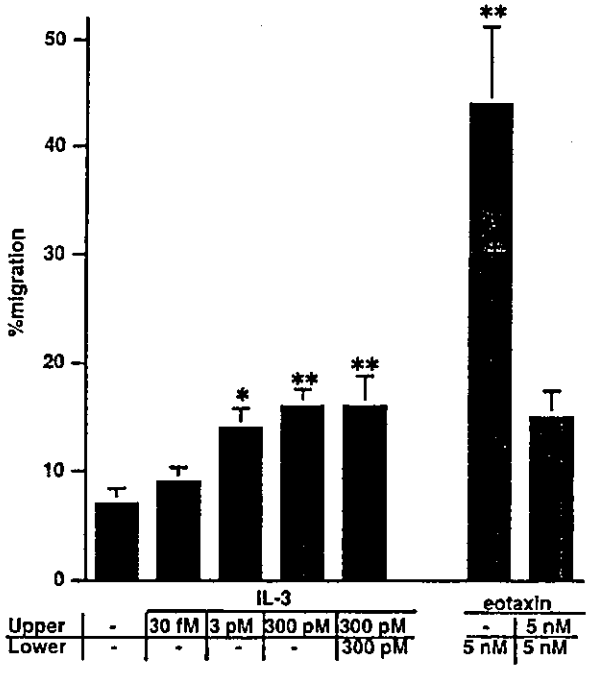

FIGURE 4. Effects of IL-3 on basophil TEM. HUVEC were treated with IL-1-β (5 ng/ml) at 37°C for 4 h. IL-3 and eotaxin (5 nM) were added to the upper and/or lower wells as indicated. Basophils were separated by Percoll, and TEM assay was performed at 37°C for 3 h. Bars represent the SEM ($n = 8$). *, $p < 0.05$; **, $p < 0.01$ (vs spontaneous migration without IL-3 or eotaxin).

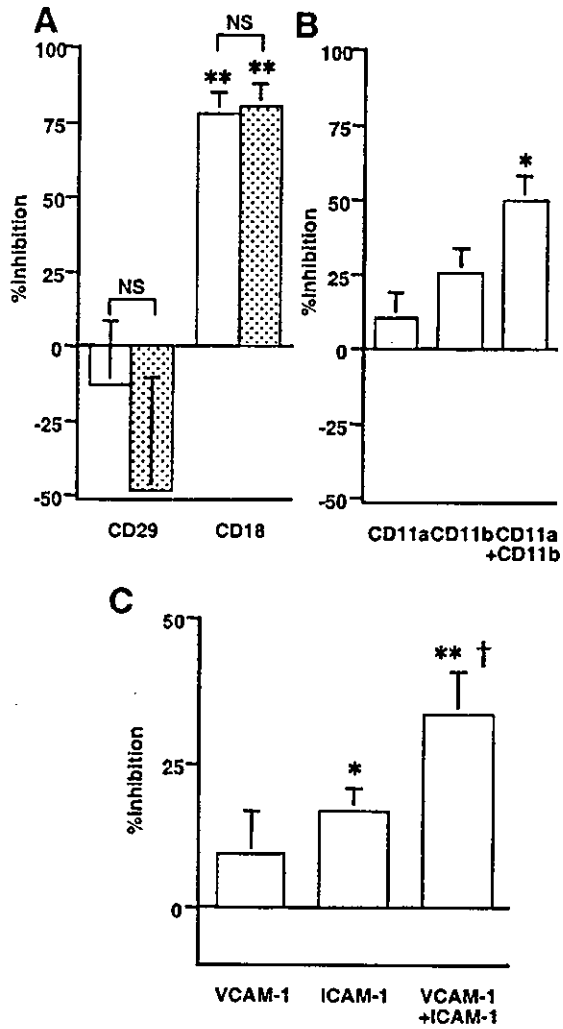

FIGURE 5. Effects of adhesion molecules on spontaneous basophil TEM across activated HUVEC. *A*, HUVEC were pretreated with IL-1-β (5 ng/ml) at 37°C for 4 h. Percoll-separated (□) and MACS-separated (□) basophils were preincubated with anti-adhesion molecule mAb (10 μg/ml) or isotype control mAb (mouse IgG1) at 37°C for 30 min. The TEM assay was performed at 37°C for 3 h. Bars represent the SEM ($n = 4$). The purities of Percoll- and MACS-separated basophils were 17.6 ± 3.7 and 98.8 ± 0.9%, respectively. Control migrations of Percoll-separated and highly purified basophils pretreated with control mAb were 4.6 ± 1.8 and 3.3 ± 1.6%, respectively. *, $p < 0.05$; **, $p < 0.01$ (vs control migration). NS, no significant difference between Percoll-separated and highly purified basophils. *B*, HUVEC were pretreated with IL-1β (5 ng/ml) at 37°C for 4 h. Percoll-separated basophils were preincubated with anti-adhesion molecule mAb (10 μg/ml) or isotype control mAb (mouse IgG1) at 37°C for 30 min. The TEM assay was performed at 37°C for 3 h. Bars represent the SEM ($n = 8$–10). Control migration of basophils pretreated with control mAb was 7.3 ± 1.1%. *, $p < 0.05$; **, $p < 0.01$ (vs control migration). *C*, IL-1-stimulated HUVEC were pretreated with the $F(ab')_2$ of anti-VCAM-1 mAb (3 μg/ml), anti-ICAM-1 mAb (10 μg/ml), or control Ab (mouse IgG, 10 μg/ml) at 37°C for 30 min. The TEM assay was performed using Percoll-separated basophils at 37°C for 3 h. Bars represent the SEM ($n = 6$). Control migration across HUVEC precultured with the $F(ab')_2$ of control Ab was 9.5 ± 1.8%. *, $p < 0.05$; **, $p < 0.01$ (vs control migration). †, $p < 0.05$ (vs migration after pretreatment with anti-ICAM-1 mAb).

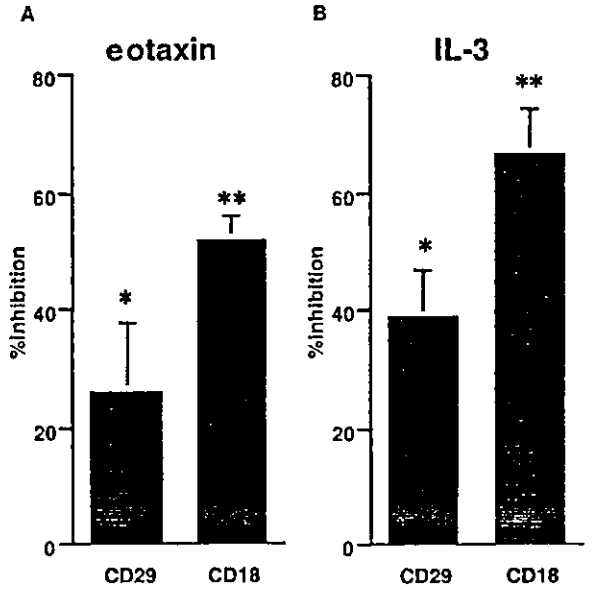

FIGURE 6. Effects of adhesion molecules on eotaxin-mediated (*A*) and IL-3-mediated (*B*) basophil TEM across activated HUVEC. HUVEC were pretreated with IL-1-β (5 ng/ml) at 37°C for 4 h. *A*, Percoll-separated basophils were treated with anti-CD18 mAb (10 μg/ml), anti-CD29 mAb (10 μg/ml), or isotype control mAb (10 μg/ml) at 37°C for 30 min. TEM assay was performed at 37°C for 3 h in the presence of eotaxin (5 nM) in the lower wells. *B*, Percoll-separated basophils were preincubated with IL-3 (300 pM) at 37°C for 30 min plus anti-CD18 mAb (10 μg/ml), anti-CD29 mAb (10 μg/ml), or isotype control mAb (10 μg/ml) at 37°C for 30 min. Basophil TEM was performed at 37°C for 3 h. Bars represent the SEM (n = 6–8). Control migrations induced by eotaxin and IL-3 in the case of basophils pretreated with isotype control mAb were 22.7 ± 7.6 and 22.4 ± 3.4%, respectively. Spontaneous TEM without eotaxin or IL-3 was 8.6 ± 1.7%. *, $p < 0.05$; **, $p < 0.01$ (vs control migration).

with a combination of both mAbs resulted in significant inhibition of basophil TEM (Fig. 5*B*). In contrast, as expected, neither anti-CD49d nor anti-CD49e mAb inhibited TEM (−14.6 ± 24.3 and −37.5 ± 26.8%, inhibitory effects of anti-CD49d and anti-CD49e mAb, respectively; n = 7). Fig. 5*C* depicts the effects of counter-receptors of endothelial cells on spontaneous TEM. When IL-1-stimulated HUVEC were pretreated with F(ab')$_2$ of anti-CD106 (VCAM-1) or anti-CD54 (ICAM-1) mAb, we found that TEM of fresh basophils was significantly inhibited by anti-ICAM-1 mAb alone. Although anti-VCAM-1 mAb alone failed to exert a significant inhibitory effect, the combination of anti-VCAM-1 and anti-ICAM-1 mAbs produced enhanced inhibition compared with anti-ICAM-1 alone, indicating an additive inhibitory effect of anti-VCAM-1 mAb. Taken together, these results indicate that the β_2 integrin/ICAM-1 system is mainly responsible for TEM of fresh basophils across activated HUVEC, in which the β_1 integrin/VCAM-1 system may also play an additive role.

In contrast to spontaneous TEM, eotaxin-induced TEM was significantly inhibited not only by anti-CD18 mAb, but also by anti-CD29 mAb (Fig. 6*A*). The inhibition by anti-CD29 mAb was significantly less prominent than that by anti-CD18 mAb. TEM of IL-3-primed basophils was also inhibited by anti-CD29 mAb, although again less potently than with anti-CD18 mAb. These results indicate that β_1 integrins are more actively involved in eotaxin- or IL-3-induced basophil TEM, in contrast to spontaneous TEM.

Discussion

Participation of basophils in allergic inflammation has been strongly inferred from both the increase in the number of these cells and the presence of basophil-derived mediators at inflammatory sites during allergic reactions (2–6, 9). TEM represents an essential step for movement of leukocytes from the circulation to inflamed tissue sites, and numerous reports have extensively studied TEM of various types of leukocytes (26). In contrast, to our knowledge no studies have dealt with basophil TEM to date. In the present study, using well-established assay systems, for the first time we have investigated basophil migration across vascular endothelial cell monolayers.

The chemokine family has been highly implicated in the pathogenesis of inflammation of various etiologies (27). In addition, several lines of evidence have demonstrated that chemokines play an important role in TEM of various leukocytes (28–31). The same situation was observed in TEM of basophils. We previously studied the expression profile and functions of chemokine receptors in human basophils (13). CCR3 is constitutively expressed on the basophil surface, and CCR3 ligands such as eotaxin induced the most potent migratory responses in freshly isolated basophils. In contrast, although surface expression of CXCR4 is hardly detectable in freshly isolated basophils, it becomes gradually apparent during culture, and SDF-1 induces a strong migratory response, comparable to that induced by eotaxin (13). In parallel to these previous findings, our present results show the involvement of both CCR3 and CXCR4 in basophil TEM; strong TEM was induced by CCR3 ligands in freshly isolated cells and by SDF-1 in 24-h cultured basophils (Fig. 2*B*). The physiological role of CXCR4 on basophils is uncertain at present. However, as discussed in our previous paper (13), constitutive and ubiquitous expression of SDF-1 in many tissues suggests that CXCR4 is involved, rather, in baseline trafficking of basophils. In the present study we found that CCR2, which is strongly expressed on basophils (13, 16), is also actively involved in basophil TEM. Our earlier report showed that whereas CCR2 causes the most potent degranulation of basophils (13), its migration-inducing ability is only marginal. Based on the numbers of migrated basophils, MCP-1 is ~5-fold less potent than eotaxin (13). In contrast to those findings, the present study demonstrated that MCP-1 elicited strong basophil TEM, comparable to that induced by eotaxin. This observation is of potential importance, because CCR2 is virtually undetectable on human eosinophils (32), and MCP-1 fails to induce eosinophil TEM at all (29). As discussed below, many of the regulatory mechanisms of TEM of basophils are shared with eosinophils. Therefore, MCP-1-mediated basophil TEM may represent a unique mechanism for selective migration of human basophils. In contrast, we failed to observe any significant direct effects of CCR1, CCR2, CCR5, CXCR1, and CXCR2 on basophil TEM. Thus, although we cannot exclude possible additional effects of these receptors, it is reasonably concluded that basophil TEM is regulated mainly by both CCR2 and CCR3, and by CXCR4 under certain circumstances.

HUVEC are capable of liberating various chemokines in response to diverse stimuli (33–35). Therefore, it should be noted that HUVEC-derived chemokines might disturb the chemotactic gradient and thereby affect the TEM results. Furthermore, more complicated mechanisms may exist regarding the CXCR4/SDF-1 system; Murdoch et al. (36) reported that HUVEC expressed CXCR4 and induced a rapid calcium influx in response to SDF-1. Inasmuch as CXCR4 on vascular endothelial cells is up-regulated by activating stimuli, the presence of SDF-1 may induce and/or modulate cytokine/chemokine production by activated HUVEC. Even though we stimulated HUVEC for only a short time (4 h) and eliminated possible soluble factors from HUVEC by washing before performing TEM assays, there remains the possibility that HUVEC-derived mediators might affect the TEM results, as reported for eosinophil TEM (34).

We and others have demonstrated that IL-3 represents the most potent basophil-activating cytokine and stimulates various aspects of basophil functions, including mediator release (21, 22), survival (23, 24), motility (11), adhesiveness to the endothelium (14), and expression of activation markers (14). Our present finding that IL-3 potentiated basophil TEM broadens the current concept of the capacity of IL-3 to modulate allergic inflammatory responses by up-regulating basophil functions. However, it seems unlikely that IL-3 is directly involved in basophil accumulation at allergic inflammatory sites, because checkerboard analyses clearly showed that IL-3-mediated TEM was chemokinetic rather than chemotactic. Nevertheless, the additive effect of IL-3 seen in eotaxin-induced TEM strongly suggested that IL-3, and potentially IL-5 and GM-CSF as well, plays a cooperative role in basophil TEM with these basophil-directed chemokines by modulating locomotive movement.

In addition to basophil-directed cytokines and chemokines, adhesion molecules play a critical role in basophil TEM. Although basophils express both β_1 and β_2 integrins (12), we found that β_2 integrins represent the first line of adhesion molecules that account for basophil TEM. TEM of fresh basophils across activated HUVEC was significantly attenuated by treatment with anti-CD18 mAb. Cotreatment with anti-CD11a and anti-CD11b mAbs showed additive inhibitory effects, indicating the involvement of both the α_L and α_M chains in basophil TEM. In line with these observations, pretreatment of activated HUVEC with mAb against ICAM-1, a counter-receptor for both CD11a and CD11b, significantly inhibited basophil TEM. Furthermore, basophil TEM induced by IL-3 or eotaxin was also suppressed by anti-CD18 mAb. An in vitro study by others showed up-regulation of the expression of a β_2 integrin (CD11b) by IL-3 (14). We found that CD11b and CD18 were also up-regulated by IL-3, and that eotaxin exerted the same effect to a lesser extent (M. Iikura and K. Hirai, unpublished observation). Thus, the enhanced TEM observed in IL-3- and eotaxin-treated cells can be attributed at least in part to strengthened interaction with β_2 integrin caused by up-regulated expression of these molecules.

Our results indicated an additional role of β_1 integrins in basophil TEM. Spontaneous TEM across activated HUVEC was not inhibited by anti-CD49d, anti-49e, or anti-CD29 mAb (Fig. 5*A*), but anti-CD29 mAb significantly inhibited TEM of eotaxin- and IL-3-stimulated basophils (Fig. 6). The increase in the involvement of β_1 integrin in these cells is potentially mediated by functional up-regulation of β_1 integrin. Sung et al. (37) reported that short term incubation of eosinophils with eotaxin or GM-CSF (30 min) up-regulates the binding of cells to VCAM-1 without affecting the expression level of VLA-4 protein. Although not proven, a conformational change in the VLA-4 receptor is likely to be responsible for the increased involvement of β_1 integrin in basophils stimulated with either eotaxin or IL-3. Because β_1 integrin is specifically expressed on basophils and eosinophils, but not neutrophils (38), this molecule is strongly implicated in the selective accumulation of basophils as well as eosinophils at allergic inflammatory sites.

The results of blocking experiments showed a discrepancy in the efficacy between inhibition of α and β subunits as well as counter-receptors and leukocyte integrins. This discrepancy strongly suggests additional involvement of untested adhesion molecules in basophil TEM. Although our present results indicated essential roles for α_L and α_M in basophil TEM, the blockade of the β subunit (CD18) was more effective than that of a combination of CD11a plus CD11b (Fig. 5, *A* and *B*). The lower efficacy of blockade of α subunits indicates possible roles for other members of α subunits of β_2 integrin, i.e., CD11c (α_X) and α_d, which have been shown to be constitutively expressed on basophils (39, 40). A similar situation was postulated for counter-receptors of Ig superfamily members. We found that anti-VCAM-1 mAb showed an additive inhibitory effect in combination with anti-ICAM-1 mAb on TEM of fresh basophils regardless of the inefficacy of anti-CD29 treatment (Fig. 5, *A* and *C*). Because $\alpha_d\beta_2$ integrins use VCAM-1 as one of their counter-receptors (41), an additive role for VCAM-1 may also support the involvement of $\alpha_d\beta_2$ integrins in spontaneous basophil TEM. Furthermore, our finding that blockade of counter-receptors is markedly less effective than that of leukocyte integrins (Fig. 5, *A* and *C*) may reflect the involvement of other untested Ig superfamily members, such as ICAM-2. Additional study is required to elucidate the possible roles of these molecules in basophil TEM.

The increased TEM observed in IL-1-stimulated HUVEC indicated the importance of endothelial cell activation in basophil TEM. Throughout our experiments we used HUVEC stimulated with IL-1β for 4 h, which up-regulates mainly ICAM-1 expression (42). However, the expression profile of counter-receptors on endothelial cells varies in a stimulus- and time-dependent fashion. Furthermore, phenotypic and functional heterogeneity of vascular endothelial cells is observed among different tissues. For example, IL-4 selectively induces VCAM-1 expression in HUVEC (43) or nasal polyp-derived microvascular endothelium (44), but not in microvascular endothelial cells from skin (45), intestine (46), or lung (47). In contrast, VCAM-1 expression of pulmonary microvascular endothelial cells was selectively up-regulated by long term (24-h) stimulation with TNF-α (47). Thus, it is highly likely that basophil TEM across endothelial cells obtained from other organs and/or stimulated with other cytokines would show a different profile from our present results derived using IL-1-activated HUVEC. To elucidate the precise mechanisms of basophil TEM in various allergic diseases, basophil TEM across these endothelial cells is an important issue meriting additional investigation.

Substantial evidence to date has clearly indicated a close relationship between basophils and eosinophils (48). Both cell types share a majority of their cell surface structures, including cytokine/chemokine receptors and adhesion molecules. The activating hemopoietins for both cells, i.e., IL-3, GM-CSF, and IL-5, completely overlap, and CCR3 induces strong migratory responses of basophils as well as eosinophils. Furthermore, in contrast to neutrophils, β_1 integrins in addition to β_2 integrins are specifically expressed on the surface of both cells. The results of the present study clearly show that the regulatory profile of basophil TEM is very similar to that reported for eosinophils (19, 29, 31, 49, 50). In addition to regulatory cytokines and chemokines, adhesion molecules are also involved in TEM of basophils in a quite similar fashion as in TEM of eosinophils. These common aspects of TEM determined in vitro strongly suggest similarity of the in vivo kinetics of these two cell types.

In summary, for the first time we have studied the profile and regulation of basophil TEM using IL-1-activated HUVEC. Basophil-activating hemopoietin IL-3 and basophil-directed chemokines, such as CCR2 and CCR3 ligands, are critically involved in TEM of basophils. Although β_2 integrin/ICAM-1 plays a major role in basophil TEM, β_1 integrin/VCAM-1 clearly plays an additional role. These profiles of the regulation of basophil TEM are very similar to those of eosinophil TEM, except for that by CCR2 ligand MCP-1. Our results thus support the previous argument for a close relationship between basophils and eosinophils, and suggest similar in vivo kinetics for these two cell types.

Acknowledgments

We thank M. Imanishi and C. Tamura for their skilled technical assistance. Thanks are also extended to S. Takeyama for her excellent secretarial help.

References

1. Schroeder, J. T., D. W. MacGlashan, Jr., and L. M. Lichtenstein. 2001. Human basophils: mediator release and cytokine production. *Adv. Immunol. 77:93.*
2. Naclerio, R. M., D. Proud, A. G. Togias, N. F. Adkinson, Jr., D. A. Meyers, A. Kagey-Sobotka, M. Plaut, P. S. Norman, and L. M. Lichtenstein. 1985. Inflammatory mediators in late antigen-induced rhinitis. *N. Engl. J. Med. 313:65.*
3. Charlesworth, E. N., A. F. Hood, N. A. Soter, A. Kagey-Sobotka, P. S. Norman, and L. M. Lichtenstein. 1989. Cutaneous late-phase response to allergen: mediator release and inflammatory cell infiltration. *J. Clin. Invest. 83:1519.*
4. Lichtenstein, L. M., and B. S. Bochner. 1991. The role of basophils in asthma. *Ann. NY Acad. Sci. 629:48.*
5. Iliopoulos, O., F. M. Baroody, R. M. Naclerio, B. S. Bochner, A. Kagey-Sobotka, and L. M. Lichtenstein. 1992. Histamine-containing cells obtained from the nose hours after antigen challenge have functional and phenotypic characteristics of basophils. *J. Immunol. 148:2223.*
6. Guo, C. B., M. C. Liu, S. J. Galli, B. S. Bochner, A. Kagey-Sobotka, and L. M. Lichtenstein. 1994. Identification of IgE-bearing cells in the late-phase response to antigen in the lung as basophils. *Am. J. Respir. Cell Mol. Biol. 10:384.*
7. Irani, A. M., C. Huang, H. Z. Xia, C. Kepley, A. Nafie, E. D. Fouda, S. Craig, B. Zweiman, and L. B. Schwartz. 1998. Immunohistochemical detection of human basophils in late-phase skin reactions. *J. Allergy Clin. Immunol. 101:354.*
8. Ying, S., D. S. Robinson, Q. Meng, L. T. Barata, A. R. McEuen, M. G. Buckley, A. F. Walls, P. W. Askenase, and A. B. Kay. 1999. C-C chemokines in allergen-induced late-phase cutaneous responses in atopic subjects: association of eotaxin with early 6-hour cosinophils, and of eotaxin-2 and monocyte chemoattractant protein-4 with the later 24-hour tissue cosinophilia, and relationship to basophils and other C-C chemokines (monocyte chemoattractant protein-3 and RANTES). *J. Immunol. 163:3976.*
9. Gauvreau, G. M., J. M. Lee, R. M. Watson, A. M. Irani, L. B. Schwartz, and P. M. O'Byrne. 2000. Increased numbers of both airway basophils and mast cells in sputum after allergen inhalation challenge of atopic asthmatics. *Am. J. Respir. Crit. Care Med. 161:1473.*
10. Bochner, B. S., P. T. Peachell, K. E. Brown, and R. P. Schleimer. 1988. Adherence of human basophils to cultured umbilical vein endothelial cells. *J. Clin. Invest. 81:1355.*
11. Yamaguchi, M., K. Hirai, S. Shoji, T. Takaishi, K. Ohta, Y. Morita, S. Suzuki, and K. Ito. 1992. Haemopoietic growth factors induce human basophil migration in vitro. *Clin. Exp. Allergy 22:379.*
12. Bochner, B. S., S. A. Sterbinsky, M. Briskin, S. S. Saini, and D. W. MacGlashan, Jr. 1996. Counter-receptors on human basophils for endothelial cell adhesion molecules. *J. Immunol. 157:844.*
13. Iikura, M., M. Miyamasu, M. Yamaguchi, H. Kawasaki, K. Matsushima, M. Kitaura, Y. Morita, O. Yoshie, K. Yamamoto, and K. Hirai. 2001. Chemokine receptors in human basophils: inducible expression of functional CXCR4. *J. Leukocyte Biol. 70:113.*
14. Bochner, B. S., A. A. McKelvey, S. A. Sterbinsky, J. E. Hildreth, C. P. Derse, D. A. Klunk, L. M. Lichtenstein, and R. P. Schleimer. 1990. IL-3 augments adhesiveness for endothelium and CD11b expression in human basophils but not neutrophils. *J. Immunol. 145:1832.*
15. Yamada, H., K. Hirai, M. Miyamasu, M. Iikura, Y. Misaki, S. Shoji, T. Takaishi, T. Kasahara, Y. Morita, and K. Ito. 1997. Eotaxin is a potent chemotaxin for human basophils. *Biochem. Biophys. Res. Commun. 231:365.*
16. Uguccioni, M., C. R. Mackay, B. Ochensberger, P. Loetscher, S. Rhis, G. J. LaRosa, P. Rao, P. D. Ponath, M. Baggiolini, and C. A. Dahinden. 1997. High expression of the chemokine receptor CCR3 in human blood basophils: role in activation by eotaxin, MCP-4, and other chemokines. *J. Clin. Invest. 100:1137.*
17. Sato, K., H. Kawasaki, H. Nagayama, R. Seizawa, J. Ikeda, C. Morimoto, K. Yasunaga, N. Yamaji, K. Tadokoro, T. Juji, et al. 1999. CC chemokine receptors, CCR-1 and CCR-3, are potentially involved in antigen-presenting cell function of human peripheral blood monocyte-derived dendritic cells. *Blood 93:34.*
18. Iikura, M., M. Yamaguchi, T. Fujisawa, M. Miyamasu, T. Takaishi, Y. Morita, T. Iwase, I. More, K. Yamamoto, and K. Hirai. 1998. Secretory IgA induces degranulation of IL-3-primed basophils. *J. Immunol. 161:1510.*
19. Ebisawa, M., B. S. Bochner, S. N. Georas, and R. P. Schleimer. 1992. Eosinophil transendothelial migration induced by cytokines. I. Role of endothelial and eosinophil adhesion molecules in IL-1β-induced transendothelial migration. *J. Immunol. 149:4021.*
20. Ochensberger, B., L. Tassera, D. Bifrare, S. Rihs, and C. A. Dahinden. 1999. Regulation of cytokine expression and leukotriene formation in human basophils by growth factors, chemokines and chemotactic agonists. *Eur. J. Immunol. 29:11.*
21. Hirai, K., Y. Morita, Y. Misaki, K. Ohta, T. Takaishi, S. Suzuki, K. Motoyoshi, and T. Miyamoto. 1988. Modulation of human basophil histamine release by hemopoietic growth factors. *J. Immunol. 141:3958.*
22. Kurimoto, Y., A. L. de Week, and C. A. Dahinden. 1989. Interleukin 3-dependent mediator release in basophils triggered by C5a. *J. Exp. Med. 170:467.*
23. Yamaguchi, M., K. Hirai, Y. Morita, T. Takaishi, K. Ohta, S. Suzuki, K. Motoyoshi, O. Kawanami, and K. Ito. 1992. Hemopoietic growth factors regulate the survival of human basophils in vitro. *Int. Arch. Allergy Immunol. 97:322.*
24. Miura, K., S. S. Saini, G. Gauvreau, and D. W. MacGlashan, Jr. 2001. Differences in functional consequences and signal transduction induced by IL-3, IL-5, and nerve growth factor in human basophils. *J. Immunol. 167:2282.*
25. Fureder, W., H. Agis, W. R. Sperr, K. Lechner, and P. Valent. 1994. The surface membrane antigen phenotype of human blood basophils. *Allergy 49:861.*
26. Luscinskas, F. W., S. Ma, A. Nusrat, C. A. Parkos, and S. K. Shaw. 2002. Leukocyte transendothelial migration: a junctional affair. *Semin. Immunol. 14:105.*
27. Gerard, C., and B. J. Rollins. 2001. Chemokines and disease. *Nat. Immunol. 2:108.*
28. Smith, W. B., J. R. Gamble, I. Clark-Lewis, and M. A. Vadas. 1991. Interleukin-8 induces neutrophil transendothelial migration. *Immunology 72:65.*
29. Ebisawa, M., T. Yamada, C. Bickel, D. Klunk, and R. P. Schleimer. 1994. Eosinophil transendothelial migration induced by cytokines. III. Effect of the chemokine RANTES. *J. Immunol. 153:2153.*
30. Randolph, G. J., and M. B. Furie. 1995. A soluble gradient of endogenous monocyte chemoattractant protein-1 promotes the transendothelial migration of monocytes in vitro. *J. Immunol. 155:3610.*
31. Shahabuddin, S., P. Ponath, and R. P. Schleimer. 2000. Migration of eosinophils across endothelial cell monolayers: interactions among IL-5, endothelial-activating cytokines, and C-C chemokines. *J. Immunol. 164:3847.*
32. Nagase, H., M. Miyamasu, M. Yamaguchi, T. Fujisawa, K. Ohta, K. Yamamoto, Y. Morita, and K. Hirai. 2000. Expression of CXCR4 in eosinophils: functional analyses and cytokine-mediated regulation. *J. Immunol. 164:5935.*
33. Miyamasu, M., T. Nakajima, Y. Misaki, S. Izumi, N. Tsuno, T. Kasahara, K. Yamamoto, Y. Morita, and K. Hirai. 1999. Dermal fibroblasts represent a potent major source of human eotaxin: in vitro production and cytokine-mediated regulation. *Cytokine 11:751.*
34. Cuvelier, S. L., and K. D. Patel. 2001. Shear-dependent eosinophil transmigration on interleukin 4-stimulated endothelial cells: a role for endothelium-associated eotaxin-3. *J. Exp. Med. 194:1699.*
35. Komiya, A., H. Nagase, H. Yamada, T. Sekiya, M. Yamaguchi, Y. Sano, N. Hanai, A. Furuya, K. Ohta, K. Matsushima, et al. 2003. Concerted expression of eotaxin-1, eotaxin-2, and eotaxin-3 in human bronchial epithelial cells. *Cell. Immunol. 225:91.*
36. Murdoch, C., P. N. Monk, and A. Finn. 1999. Cxc chemokine receptor expression on human endothelial cells. *Cytokine 11:704.*
37. Sung, K. P., L. Yang, J. Kim, D. Ko, G. Stachnick, D. Castaneda, J. Nayar, and D. H. Broide. 2000. Eotaxin induces a sustained reduction in the functional adhesive state of very late antigen 4 for the connecting segment 1 region of fibronectin. *J. Allergy Clin. Immunol. 106:933.*
38. Bochner, B. S., F. W. Luscinskas, M. A. Gimbrone, Jr., W. Newman, S. A. Sterbinsky, C. P. Derse-Anthony, D. Klunk, and R. P. Schleimer. 1991. Adhesion of human basophils, eosinophils, and neutrophils to interleukin 1-activated human vascular endothelial cells: contributions of endothelial cell adhesion molecules. *J. Exp. Med. 173:1553.*
39. Bochner, B. S., and S. A. Sterbinsky. 1991. Altered surface expression of CD11 and Leu 8 during human basophil degranulation. *J. Immunol. 146:2367.*
40. Grayson, M. H., M. Van der Vieren, W. M. Gallatin, P. A. Hoffman, and B. S. Bochner. 1997. Expression of a novel β_2 integrin ($\alpha_4\beta_2$) on human leukocytes and mast cells. *J. Allergy Clin. Immunol. 99:S386.*
41. Grayson, M. H., M. Van der Vieren, S. A. Sterbinsky, W. M. Gallatin, P. A. Hoffman, D. E. Staunton, and B. S. Bochner. 1998. $\alpha_9\beta_2$ integrin is expressed on human eosinophils and functions as an alternative ligand for vascular cell adhesion molecule 1 (VCAM-1). *J. Exp. Med. 188:2187.*
42. Bochner, B. S., D. A. Klunk, S. A. Sterbinsky, R. L. Coffman, and R. P. Schleimer. 1995. IL-13 selectively induces vascular cell adhesion molecule-1 expression in human endothelial cells. *J. Immunol. 154:799.*
43. Schleimer, R. P., S. A. Sterbinsky, J. Kaiser, C. A. Bickel, D. A. Klunk, K. Tomioka, W. Newman, F. W. Luscinskas, M. A. Gimbrone, Jr., B. W. McIntyre, et al. 1992. IL-4 induces adherence of human eosinophils and basophils but not neutrophils to endothelium: association with expression of VCAM-1. *J. Immunol. 148:1086.*
44. Jahnsen, F. L., P. Brandtzaeg, R. Haye, and G. Haraldsen. 1997. Expression of functional VCAM-1 by cultured nasal polyp-derived microvascular endothelium. *Am. J. Pathol. 150:2113.*
45. Swerlick, R. A., K. H. Lee, L. J. Li, N. T. Sepp, S. W. Caughman, and T. J. Lawley. 1992. Regulation of vascular cell adhesion molecule 1 on human dermal microvascular endothelial cells. *J. Immunol. 149:698.*
46. Haraldsen, G., D. Kvale, B. Lien, I. N. Farstad, and P. Brandtzaeg. 1996. Cytokine-regulated expression of E-selectin, intercellular adhesion molecule-1 (ICAM-1), and vascular cell adhesion molecule-1 (VCAM-1) in human microvascular endothelial cells. *J. Immunol. 156:2558.*
47. Yamamoto, H., J. B. Sedgwick, and W. W. Busse. 1998. Differential regulation of eosinophil adhesion and transmigration by pulmonary microvascular endothelial cells. *J. Immunol. 161:971.*
48. Hirai, K., M. Miyamasu, T. Takaishi, and Y. Morita. 1997. Regulation of the function of eosinophils and basophils. *Crit. Rev. Immunol. 17:325.*
49. Ebisawa, M., M. C. Liu, T. Yamada, M. Kato, L. M. Lichtenstein, B. S. Bochner, and R. P. Schleimer. 1994. Eosinophil transendothelial migration induced by cytokines. II. Potentiation of eosinophil transendothelial migration by cosinophil-active cytokines. *J. Immunol. 152:4590.*
50. Jia, G. Q., J. A. Gonzalo, A. Hidalgo, D. Wagner, M. Cybulsky, and J. C. Gutierrez-Ramos. 1999. Selective eosinophil transendothelial migration triggered by eotaxin via modulation of Mac-1/ICAM-1 and VLA-4/VCAM-1 interactions. *Int. Immunol. 11:1.*

Nucleosome-Specific Regulatory T Cells Engineered by Triple Gene Transfer Suppress a Systemic Autoimmune Disease[1]

Keishi Fujio,* Akiko Okamoto,* Hiroyuki Tahara,* Masaaki Abe,† Yi Jiang, † Toshio Kitamura,‡ Sachiko Hirose,† and Kazuhiko Yamamoto[2]*

The mechanisms of systemic autoimmune disease are poorly understood and available therapies often lead to immunosuppressive conditions. We describe here a new model of autoantigen-specific immunotherapy based on the sites of autoantigen presentation in systemic autoimmune disease. Nucleosomes are one of the well-characterized autoantigens. We found relative splenic localization of the stimulative capacity for nucleosome-specific T cells in (NZB × NZW)F_1 (NZB/W F_1) lupus-prone mice. Splenic dendritic cells (DCs) from NZB/W F_1 mice spontaneously stimulate nucleosome-specific T cells to a much greater degree than both DCs from normal mice and DCs from the lymph nodes of NZB/W F_1 mice. This leads to a strategy for the local delivery of therapeutic molecules using autoantigen-specific T cells. Nucleosome-specific regulatory T cells engineered by triple gene transfer (TCR-α, TCR-β, and CTLA4Ig) accumulated in the spleen and suppressed the related pathogenic autoantibody production. Nephritis was drastically suppressed without impairing the T cell-dependent humoral immune responses. Thus, autoantigen-specific regulatory T cells engineered by multiple gene transfer is a promising strategy for treating autoimmune diseases. *The Journal of Immunology,* **2004, 173: 2118–2125.**

Systemic autoimmune diseases have traditionally been treated using nonspecific immunosuppressive agents, but these agents often lead to opportunistic infections and an increased rate of malignancy. There remains the need to develop selective or specific therapies that target individual autoantigens. Several strategies have been developed as potential Ag-specific immunotherapies, such as using Ag-pulsed dendritic cells (DCs),[3] but the majority of these approaches will require further investigation (1, 2). A more detailed understanding of autoimmune diseases, including autoantigen presentation, is required for the development of reasonable immunotherapies.

Systemic lupus erythematosus (SLE) is a life-threatening autoimmune disease characterized by the production of a variety of autoantibodies (3). Anti-DNA Abs are thought to be one of the major pathogenic products of the autoimmune response (4–6). Datta and colleagues (7–9), as well as other groups (10, 11), have noted that nucleosomes could be a major immunogen for pathogenic autoantibody-inducing T cells in lupus-prone mice. Datta and coworkers (7–9) showed that the majority of pathogenic T_H clones specific for nucleosomes were capable of rapidly inducing anti-DNA autoantibody production, and that these clones were also able to induce nephritis when injected into young lupus-prone mice. Moreover, anti-nucleosome ELISAs have demonstrated better sensitivity, specificity, and diagnostic confidence with regard to human SLE than anti-DNA ELISAs. Anti-nucleosome ELISAs are also correlated with disease activity, as determined by the SLE Disease Activity Index (12, 13).

Although evidences have accumulated demonstrating the importance of nucleosomes as major pathogenic autoantigens, the cellular mechanisms for the immunological recognition of nucleosomes are poorly understood. Generalized hyperresponsiveness of B cells has been reported in both mice and human lupus (14, 15). However, these nonspecific immune disorders cannot provide a sufficient model of nuclear autoantigen-specific autoimmunity encountered in patients with lupus.

To better understand the mechanisms of autoantigen recognition, we first reconstituted nucleosome specificity by TCR gene transfer in $CD4^+$ T cells from (NZB × NZW)F_1 (NZB/W F_1) lupus model mice (3, 16). Using this model, we demonstrated an abnormal autoantigen presentation of splenic DCs. Among the lymphoid organs, this elevated autoantigen presentation of DCs was relatively localized in the spleen. We then developed a triple gene transfer system to generate autoantigen-specific regulatory cells. These regulatory cells preferentially accumulated in the spleen and suppressed the progression of the disease without obvious systemic immunosuppression.

Materials and Methods

Preparation of retroviral construct

Line 3A is a cell line from lupus-prone (SWR × NZB)F_1 (SNF1; I-$A^{d/q}$) that can recognize the immunodominant nucleosomal epitope (histone H4; aa 71–94) in the context of I-A^d (7, 8) and many other I-A molecules (8). Both TCR-α and -β cDNA fragments were synthesized using PCR based on the published sequences of line 3A (7, 8) and designated as AN3 TCR-α and -β. Vα13 and Vβ4 fragments identical to CDR1 and two sequences of line 3A were obtained from NZB splenic cDNA and an added CDR3 sequence by PCR. Jα41-Cα fragment and Jβ2.6-Cβ fragment were also obtained from NZB splenic cDNA and an added CDR3 sequence by PCR. Vα13-CDR3 fragment and CDR3-Jα41-Cα fragment were combined in a

*Department of Allergy and Rheumatology, Graduate School of Medicine, University of Tokyo, Tokyo, Japan; †Department of Pathology, Juntendo University School of Medicine, Tokyo, Japan; and ‡Division of Cellular Therapy, Advanced Clinical Research Center, Institute of Medical Science, University of Tokyo, Tokyo, Japan

Received for publication September 24, 2003. Accepted for publication May 12, 2004.

The costs of publication of this article were defrayed in part by the payment of page charges. This article must therefore be hereby marked *advertisement* in accordance with 18 U.S.C. Section 1734 solely to indicate this fact.

[1] This study was supported by grants from the Ministry of Health, Labor and Welfare and the Ministry of Education, Culture, Sports, Science and Technology of Japan.

[2] Address correspondence and reprint requests to Dr. Kazuhiko Yamamoto, Department of Allergy and Rheumatology, Graduate School of Medicine, University of Tokyo, 7-3-1 Hongo, Bunkyo-ku, Tokyo, 113-0033, Japan. E-mail address: yamamoto-tky@umin.ac.jp

[3] Abbreviations used in this paper: DC, dendritic cell; SLE, systemic lupus erythematosus; WPRE, woodchuck hepatitis virus posttranscriptional regulatory element; IRES, internal ribosomal entry site; LN, lymph node.

0022-1767/04/$02.00

subsequent "fusion" reaction in which the overlapping ends anneal, allowing the 3′ overlap of each strand to serve as a primer for the 3′ extension of the complementary strand. The resulting fusion product is amplified further by PCR. Vβ4-CDR3 fragment and CDR3-Jβ2.6-Cβ fragment were combined similarly. The full-length fragments were cloned into a pMXW retroviral vector to obtain pMXW-AN3α and pMXW-AN3β (Fig. 1*A*). pMXW is an improved vector generated by insertion of the woodchuck hepatitis virus posttranscriptional regulatory element (WPRE) (17, 18) between the *Not*I and *Sal*I sites of pMX (19). WPRE enhances expression of transgenes delivered by retroviral vectors (18), and the expression efficiency of the pMXW vector is improved 1.5 times when WPRE is inserted, compared with the efficiency of the pMX vector. Murine CTLA4Ig cDNA was synthesized by PCR as described previously (20) and was then cloned into the pMX-IRES-GFP (21). Complementary DNAs for the TCR α- and β-chains were isolated from a cDNA library of DO11.10 TCR-transgenic splenocytes and were inserted into the retroviral vector pMX to generate pMX-DOTAE and pMX-DOTBE, respectively (22).

Mice

NZB/W F_1 and BALB/c mice were obtained from Japan SLC (Shizuoka, Japan). All animal experiments were conducted in accordance with the institutional and national guidelines.

Production of retroviral supernatants and retroviral transduction

Total splenocytes were isolated and cultured for 48 h in RPMI 1640 medium supplemented with 10% FCS, 2 mM L-glutamine, 100 U/ml penicillin, 100 μg/ml streptomycin, and 5×10^{-5} M 2-ME in the presence of Con A (10 μg/ml) and IL-2 (50 ng/ml) before the transduction. Retroviral supernatants were obtained by transfection of pMXW, pMXW-AN3α, pMXW-AN3β, pMX-IRES-GFP, pMX-CTLA4Ig-IRES-GFP, pMX-DOTAE, or pMX-DOTBE DNA into PLAT-E packaging cell lines (22, 23) with the use of the FuGENE 6 transfection reagent (Roche Diagnostic Systems, Somerville, NJ).

Falcon 24-well plates (BD Biosciences, San Jose, CA) were coated with the recombinant human fibronectin fragment CH296 (Retronectin; Takara, Otsu, Japan) according to the manufacturer's instructions. Before infection, virus-bound plates were prepared. The viral supernatant (500 μl) was preloaded onto each well of the CH296-coated plate, and the plate was spun at $2000 \times g$ for 3 h at 32°C. The virus-coating procedure was repeated three times. Before infection, the viral supernatant was washed away and splenocytes prestimulated for 48 h were added to each well (1×10^6 cells/well). Cells were cultured for 36 h to allow infection to occur. To control the viral expression efficiency, we produced a viral supernatant (pMXW, pMXW-AN3α, pMXW-AN3β, pMX-IRES-GFP, and pMX-CTLA4Ig-IRES-GFP, simultaneously) and prechecked the uniformity of the infection efficiency before in vitro and in vivo experiments.

Cell purification

A $CD4^+$ T cell population was prepared by negative selection with MACS using anti-CD19 mAb, anti-CD11c, mAb, and anti-CD8a mAb. $CD11c^+$ DCs were prepared as previously described (24, 25). Briefly, spleen cells or lymph node cells were digested with collagenase type IV (Sigma-Aldrich, St. Louis, MO) and DNase I, and the $CD11c^+$ cells were selected twice by positive selection using MACS CD11c microbeads and magnetic separation columns. The purity (85% in average) was determined by visualization with anti-CD11c-biotin followed by streptavidin-PE. A $CD19^+$ B cell population was prepared by positive selection with MACS using anti-CD19 mAb. For CFSE labeling (Molecular Probes, Eugene, OR), cells were resuspended in PBS at 1×10^7/ml and incubated with CFSE at a final concentration of 5 mM for 30 min at 37°C, followed by two washes in PBS.

Nucleosome preparation

Pure nucleosomes were prepared as previously described (26). Briefly, frozen pure chicken erythrocytes were thawed and suspended in lysis buffer on ice (10 mM Tris-HCl, 10 mM NaCl, 5 mM $MgCl_2$, 0.5% Nonidet P-40, and 0.25 mM $PhMeSO_2F$, pH 7.5). The nuclei were recovered by centrifugation and the nuclear pellet was washed and digested with micrococcal nuclease. The nuclear pellet was lysed into 0.2 mM Na_2EDTA, and nuclear debris was removed by centrifugation. The soluble chromatin at $A_{260} \approx 100$ was dialyzed against 5 mM triethanolamine HCl, 60 mM NaCl, 1 mM Na_2EDTA (pH 7.5), and subsequently fractionated in the same buffer, usually in sucrose gradients. Gradients were fractionated and monitored at 280 nm, and the appropriate fractions were pooled.

Proliferation assay

At 24 h postinfection, purified $CD4^+$ T cells were cultured at 2×10^4cells/well, with 1×10^5 cells/well of irradiated $CD19^+$ B cells or 1×10^4 cells/well of irradiated $CD11c^+$ DCs in 96-well flat-bottom microtiter plates in volumes of 100 μl of complete medium with or without 1 μg/ml nucleosome or 0.3 μM chicken $OVA_{323-339}$ peptide. After 24 h of culture, the cells were pulse labeled with 1 μCi of [^{3}H]thymidine/well (NEN Life Science Products, Boston, MA) for 15 h and the [^{3}H]thymidine incorporation was determined. In some experiments, we calculated the ratio of (group A − cpm)/(group B − cpm) in each experiment and showed the average ratio of three to five experiments as "average ratio of (group A − cpm)/(group B − cpm) to clarify the reproducibility of the data.

Transfer experiments

The indicated number of cells suspended in PBS were i.v. injected into mice. For the transfer of gene-transduced cells, cell viability was always >97%, as detected by trypan blue exclusion.

ELISA

IgG anti-DNA Abs were quantified using ELISA plates coated with calf thymus DNA (Sigma-Aldrich, and the DNA-binding activities were expressed in units, referring to a standard curve obtained by serial dilutions of a standard serum pool from 7- to 9-mo-old NZB/W F_1 mice, containing 1000 U/ml. IgG antinucleosome Abs or IgG anti-histone Abs were quantified using ELISA plates coated with purified nucleosome or purified histone. Methods for detection of CTLA4Ig protein were described previously (27). Briefly, ELISA plates were coated with anti-mouse CTLA4 (BD PharMingen, San Diego, CA) overnight at 4°C, blocked with blocking solution, and then incubated sequentially for 1 h at 37°C with serial dilutions of serum or culture supernatants followed by peroxidase-conjugated $F(ab')_2$ goat anti-mouse IgG2a (Accurate Antibodies, Westbury, NY) and ABTS substrate (Kirkegaard & Perry, Gaithersburg, MD). Serial dilutions of a known concentration of purified CTLA4Ig were used in each plate to establish a standard curve.

Histopathology

Organs were fixed in 4% paraformaldehyde, embedded in paraffin, and stained with periodic acid-Schiff solution. For three-color immunofluorescence staining, sections were incubated with biotinylated peanut agglutinin (Vector Laboratories, Burlingame, CA) and then with Cy5.5-conjugated streptavidin (Cortex Biochemicals, Irvine, CA). The sections were then stained with a rat Alexa488-labeled mAb to B220 and tetramethylrhodamine-conjugated mAbs to CD4 and CD8 (Vector Laboratories). To detect the deposition of immune complexes at glomeruli, we incubated sections with FITC-labeled goat Abs to mouse IgG or to C3 (ICN Pharmaceuticals, Costa Mesa, CA).

Statistical analysis

Statistical significance was determined using the unpaired Student's *t* test or the Mann-Whitney *U* test.

Results

Transduction of nucleosome-specific AN3 TCR confers specificity for the nucleosome and autoreactivity to DCs in NZB/W F_1 $CD4^+$ T cells

We previously reported successful TCR gene transfer and reconstitution of the Ag specificity to OVA in BALB/c $CD4^+$ T cells (27). In the present study, we transferred nucleosome-specific TCR genes (AN3α and β) into NZB/W F_1 splenocytes. To improve the expression of the introduced genes, we generated a Moloney-based retroviral vector, pMXW, by insertion of the woodchuck fragment (17, 18) into pMX (19). We selected the TCR of line 3A from lupus-prone SNF1 mice. A hybridoma transfected with this TCR did not exhibit any significant response to either $H\text{-}2^d$ or $H\text{-}2^z$ APCs (28). Each TCR gene was inserted into pMXW, and the resulting retrovirus vectors (pMXW-AN3α and pMXW-AN3β) were used for the gene transfer (Fig. 1*A*).

Retroviral infection of the AN3 TCR genes into NZB/W F_1 splenocytes induced a 40–45% increase in the $V\beta4^+$ population in $CD4^+$ T cells compared with mock-infected splenocytes (Fig. 1*B*). The calculated efficiency of the Vβ4 introduction into the

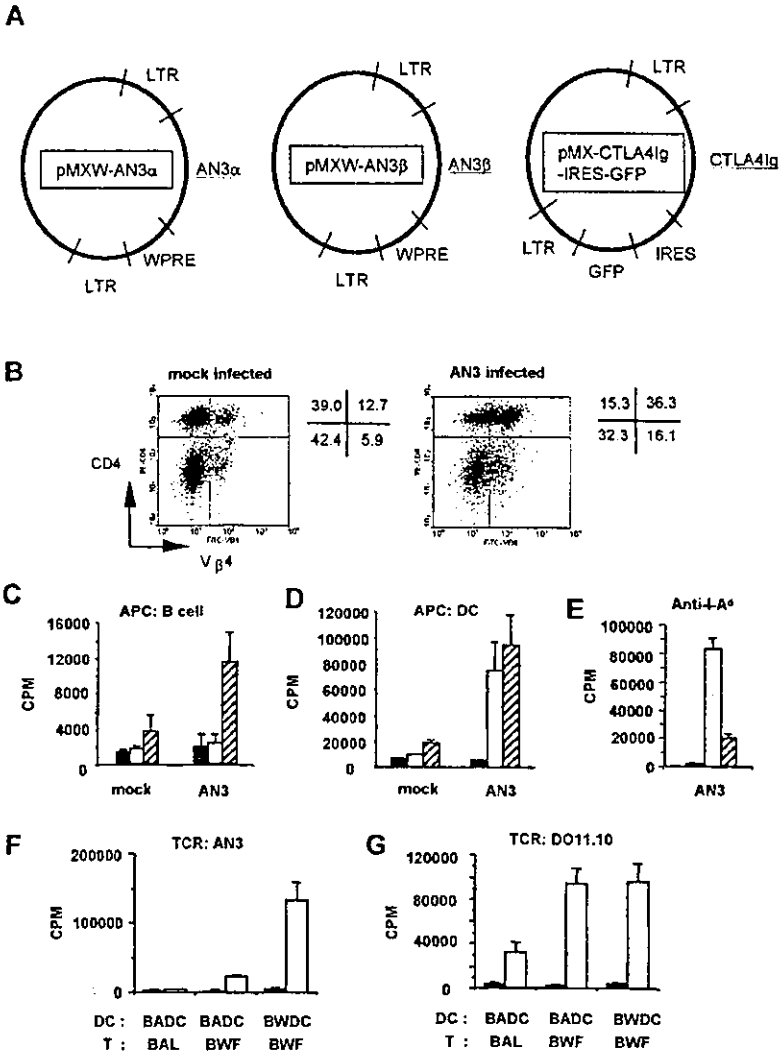

FIGURE 1. Retroviral transfer of AN3 TCR reconstituted the specificity for nucleosomes on NZB/W F_1 $CD4^+$ T cells. Reconstituted T cells showed autoreactivity to splenic DCs. *A*, Schematic representation of the pMXW retrovirus construct expressing the cDNA for the AN3 TCRα or TCRβ chain. LTR, long terminal repeat. *B*, Anti-CD4 and anti-Vβ4 staining of pMXW (mock) or AN3 TCR-transduced NZB/W F_1 splenocytes. Results of a representative experiment are shown. *C*, Proliferation of AN3-transduced and mock-transduced $CD4^+$ T cells to B cells with nucleosomes. ■, T cells alone; □, T + B; ▨, T + B + nucleosomes (1 μg/ml). *D*, Proliferation of AN3-transduced and mock-transduced $CD4^+$ T cells to $CD11c^+$ DCs with nucleosomes. ■, T cells alone; □, T + DCs; ▨, T + DCs + nucleosomes (1 μg/ml). *E*, Blockade of AN3-transduced $CD4^+$ T cell proliferation to NZB/W F_1 $CD11c^+$ DCs by an anti-I-A^d Ab, K24-199. ■, T cells alone; □, T + DCs; ▨, T + DCs + anti-I-A^d Ab. *F*, Proliferative response of AN3- or mock-transduced $CD4^+$ T cells from BALB/c (BAL) or NZB/W F_1 (BWF) (■, mock-transduced cells; □, AN3-transduced cells) with BALB/c $CD11c^+$ DCs (BADC) or NZB/W F_1 $CD11c^+$ DCs (BWDC). *G*, Proliferative response of DO11.10- and mock-transduced $CD4^+$ T cells from BALB/c (BAL) or NZB/W F_1 (BWF) (■, mock-transduced cells; □, DO11.10-transduced cells with 0.3 μM $OVA_{323-339}$) with BALB/c $CD11c^+$ DCs (BADC) or NZB/W F_1 $CD11c^+$ DCs (BWDC). Data shown are representative of more than three independent experiments with similar results.

$CD4^+V\beta4^-$ population was 50–60%. The lack of anti-Vα13 or anti-clonotypic Abs prevented direct visualization of AN3 TCR surface expression. However, based on the transduction of other TCR pairs (i.e., OVA-specific DO11.10 TCR detected by a clonotypic Ab KJ1-26; and AV8/BV7, detectable by anti-Vα8 and anti-Vβ7 Abs; data not shown), we speculate that Vα chain expression is approximately equal to that of the Vβ chain. Thus, the proportion of clonotypic AN3 TCR-expressing cells was estimated to be 25–36% in $CD4^+$ T cells. These cells were referred to as BWF.AN3, and the mock-infected $CD4^+$ T cells were referred to as BWF.mock.

We investigated the specific reactivity to the nucleosomes of BWF.AN3 in the presence of NZB/W F_1 B cells and DCs. Although BWF.mock cells showed minimal proliferation in the presence of B cells and the nucleosomes, BWF.AN3 showed strong proliferation in the presence of B cells and the nucleosomes, but not in the presence of B cells alone (Fig. 1*C*). The average ratio of (BWF.AN3 - cpm)/(BWF.mock − cpm) was 1.13 ± 0.12 and that of (BWF.AN3 with nucleosome (nuc) − cpm)/(BWF.mock with nuc − cpm) was 3.12 ± 0.51 in three experiments ($p < 0.005$). These results demonstrate that the introduction of AN3 TCR reconstitutes the specificity for the nucleosome on $CD4^+$ T cells. Furthermore, BWF.AN3 showed proliferation in the presence of splenic DCs without nucleosome (Fig. 1*D*). The average ratio of (BWF.AN3 − cpm)/(BWF.mock − cpm) was 6.97 ± 1.63 in five experiments ($p < 0.001$). Consistent with previous report that $CD4^+$ T cells of lupus-prone mice responded to nucleosome ex vivo (7), BWF.mock showed relatively weak proliferation in the presence of splenic DCs and nucleosome. The average ratio of (BWF.mock with nuc − cpm)/(BWF.mock − cpm) was 2.21 ± 0.73 in five experiments ($p < 0.05$). Despite these endogenous responses of BWF.mock to nucleosome, BWF.AN3 showed stronger proliferation compared with BWF.mock in the presence of splenic DCs with the nucleosomes. The average ratio of (BWF.AN3 with nuc − cpm)/(BWF.mock with nuc − cpm) was 4.01 ± 2.18 in five experiments ($p < 0.05$).

AN3α-infected or β-infected cells failed to respond to the DCs (data not shown), and the autoreactive response was blocked by anti-I-A^d Ab (Fig. 1*E*). Thus, this autoreactivity of BWF.AN3 to splenic DCs suggests that NZB/W F_1 splenic DCs spontaneously present a considerable amount of nucleosomal epitopes.

The nucleosome-specific response of NZB/W F_1 mice consisted of general T cell hyperreactivity and Ag-specific hyperpresentation of splenic DCs

To investigate the relative contribution of either T cells or splenic DCs to the autoreactive response, we also transduced the AN3 TCR into BALB/c $CD4^+$ T cells and these cells were referred to

as BAL.AN3. Although BAL.AN3 showed no proliferative response to BALB/c splenic DCs, BWF.AN3 showed a moderate proliferative response to BALB/c splenic DCs (Fig. 1*F*). These results suggest that the BWF1 T cell hyperreactivitiy enables BWF.AN3 to recognize small amounts of nucleosomal epitope presented on BALB/c splenic DCs, but these small amounts are ignored by BAL.AN3. As expected, BWF.AN3 strongly responded to BWF1 splenic DCs. Proliferative response of BWF.AN3 in the presence of BALB/c splenic DCs amounted to ~14–18% of that to BWF1 splenic DCs, indicating that the abnormal presentation of splenic DCs may contribute more to the autoreactive response than does T cell hyperreactivity.

To determine the general Ag recognition and reactivity of NZB/W F_1 mice, we examined the proliferation of T cells transduced with OVA-specific TCR (DO11.10). Fifty to 60% of the total $CD4^+$ T cells expressed the introduced DO11.10 TCR, as determined by the anti-clonotypic Ab KJ1-26. DO11.10-transduced BWF1 T cells cultured with DCs plus $OVA_{323-339}$ peptide exhibited stronger proliferation than BALB/c T cells, again suggesting that BWF1 T cells possess general hyperreactivity. In contrast, the OVA peptide-presentation (Fig. 1*G*) and the whole OVA presentation (data not shown) of NZB/W F_1 splenic DCs appeared to be quite similar to that of BALB/c splenic DCs. Thus, the hyperpresentation of DCs seems to be restricted to a certain Ag.

Nucleosome-specific T cells interacted with the autoantigen in the spleen

DCs in every type of lymphoid tissue may present nucleosomal epitopes, because nucleosomal Ags are available in every organ. To investigate this possibility, we fluorescently labeled either BWF.mock or BWF.AN3 T cells in vitro with CFSE and injected them into NZB/W F_1 mice. Two days after the transfer, T cells from the spleen and those from the peripheral lymph nodes (LNs) were harvested and analyzed. BWF.mock isolated from the spleen exhibited a convergent strong fluorescence peak, indicating that these cells had not proliferated extensively. In contrast, BWF.AN3 isolated from the spleen exhibited several weaker fluorescence peaks. Moreover, AN3 $CD4^+$ T cells underwent multiple divisions over a 5-day period of the experiment, and mock $CD4^+$ T cells underwent a very slight progression of cell division (Fig. 2*A*). These findings suggested that BWF.AN3 encountered the nucleosomal epitope in the spleen. It was of note that both CFSE-labeled BWF.mock and BWF.AN3 isolated from the peripheral LNs exhibited a strong convergent fluorescence peak, suggesting that BWF.AN3 encountered the nucleosomal epitope less frequently in the LNs.

A comparison of the stimulative capacity for BWF.AN3 also suggested that splenic DCs presented more nucleosomal epitope than DCs from the peripheral LNs (Fig. 2*B*). The average ratio of (BWsplDC − cpm)/(BWLNDC − cpm) was 2.79 ± 0.44 in three experiments ($p < 0.005$). These results showed that nucleosome-specific T cells are stimulated predominantly in the spleen.

Effect of CTLA4Ig transfer on the nucleosomal response

We next tried to generate nucleosome-specific regulatory cells by introducing an immunosuppressive molecule, CTLA4Ig, as the third gene in BWF.AN3 T cells. Long-term administration of CTLA4Ig to NZB/W F_1 mice has been shown to prevent disease onset for a period of months (29).

We constructed a pMX-CTLA4Ig-IRES-GFP vector (Fig. 1*A*). We then performed a triple gene transfer of the AN3$\alpha\beta$ and CTLA4Ig genes to investigate the effect on CTLA4Ig expression. The experimental groups consisted of $CD4^+$ T cells transduced with either AN3 + CTLA4Ig-IRES-GFP(CTLA4Ig), AN3 + IRES-GFP(IG), pMXW(mock) + CTLA4Ig, or mock + IG. The average expression efficiency from several different sets of infection was 45.2% for Vβ4 and 47.3% for GFP in $CD4^+$ cells (Fig. 3*A*). The average expression efficiency is expected to be 45% for the AN3α gene, and the average percentage of GFP^+AN3^+ cells expressing all three gene products in $CD4^+$ T cells was estimated to be ~10% (0.45 × 0.45 × 0.45). As shown in Fig. 3*B*, the CTLA4Ig secreted from T cells blocked the proliferation of the endogenous T cell population to the nucleosome to a moderate degree. The average ratio of (mock + CTLA4Ig with nuc − cpm)/(mock + IG with nuc − cpm) was 0.40 ± 0.07 in three experiments ($p < 0.005$). But the T cell stimulation mediated by AN3 TCR was not blocked by CTLA4Ig. The average ratio of (AN3 + IG − cpm)/(mock + IG − cpm) was 7.85 ± 1.07 and that of (AN3 + CTLA4Ig − cpm)/(mock + IG − cpm) was 7.18 ± 0.96 in three experiments. The AN3 + CTLA4Ig transduced cells showed the increase of CTLA4Ig secretion on T cell activation in the presence of DCs (Fig. 3*C*).

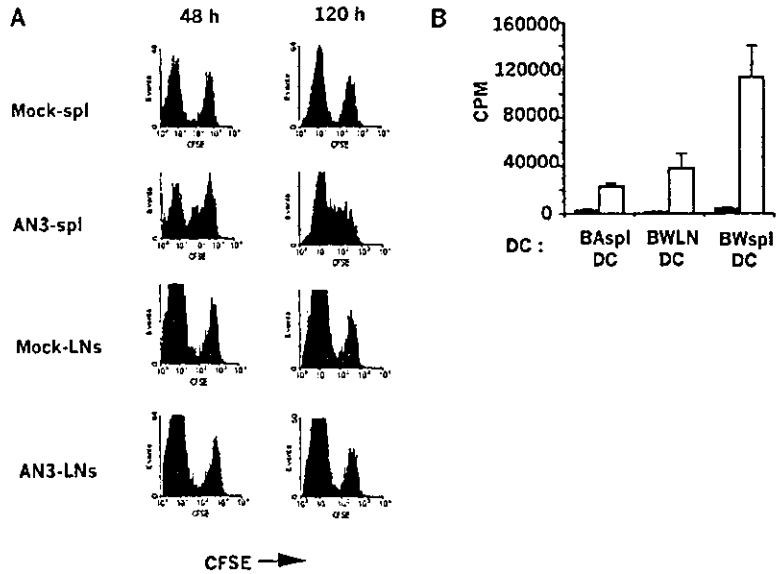

FIGURE 2. Nucleosome-specific T cells were stimulated more strongly in the spleen than in the LNs. *A*, CFSE-labeled BWF_1.mock T cells or BWF.AN3 T cells were transferred i.v. into 10-wk-old NZB/W F_1 mice. Two and 5 days later, splenocytes or peripheral LNs (cervical, inguinal, and mesenteric) from recipient mice were examined for $CFSE^+V\beta4^+$-gated cells. *B*, Proliferation of AN3- or mock-transduced T cells to $CD11c^+$ DCs from the spleen or LNs. $CD11c^+$ DCs from NZB/W F_1 spleens (BWsplDC), from NZB/W F_1 LNs (BWLNDC) and from BALB/c spleens (BAsplDC). Data shown are representative of three independent experiments with similar results.

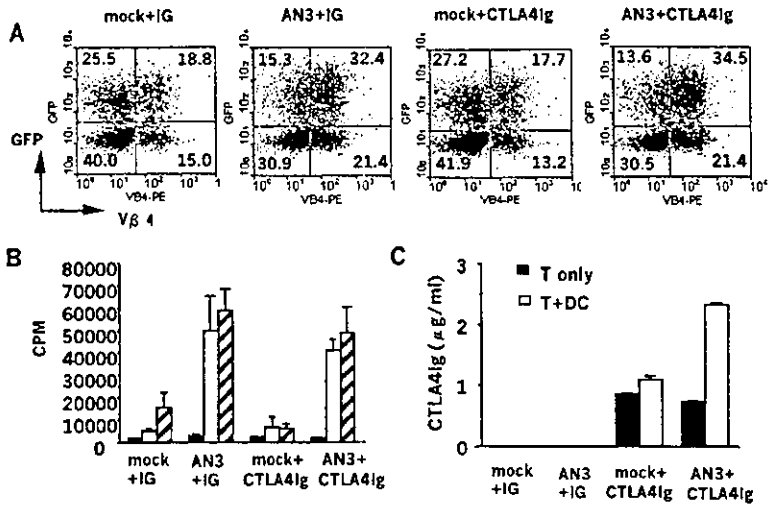

FIGURE 3. Effect of CTLA4Ig gene transfer on the T cell proliferation to nucleosomes. *A*, Expression analysis of GFP and Vβ4 in gene-transduced cells gated for CD4. The transduction efficiency was ~45% for a single gene in each group. *B*, Suppressive effect of CTLA4Ig transduction on T cell activation to nucleosomes. ■, T cells alone; □, T + DCs; ▨, T + DCs + nucleosome. *C*, CTLA4Ig production of T cells with or without DCs. Each culture supernatant was harvested after 24 h of culture. Data shown are representative of three independent experiments with similar results.

Nucleosome-specific regulatory cells suppressed autoimmune disease

We transferred cell suspensions containing 1×10^6 cells of $CD4^+$ T cells, calculatedly expressing either AN3 + CTLA4Ig, AN3 + IG, mock + CTLA4Ig, or mock + IG into 10-wk-old NZB/W F_1 mice.

The autoantibodies usually found in NZB/W F_1 mice were measured in the sera from the different groups. The elevations of anti-dsDNA and anti-histone Abs were suppressed in AN3 + CTLA4Ig-injected mice at 22 wk of age (Fig. 4*A*). AN3 + CTLA4Ig-injected mice showed the lowest average titer of anti-nucleosome Ab, but the titer in this group was not significantly different from those in the controls. This inefficient suppression may be due to the fact that autoimmunity to the nucleosome is the driving reaction and that this reaction is stronger than the subsequent response.

The mice were monitored biweekly for proteinuria. By week 22, control mice that had received PBS, mock + IG, AN3 + IG, or

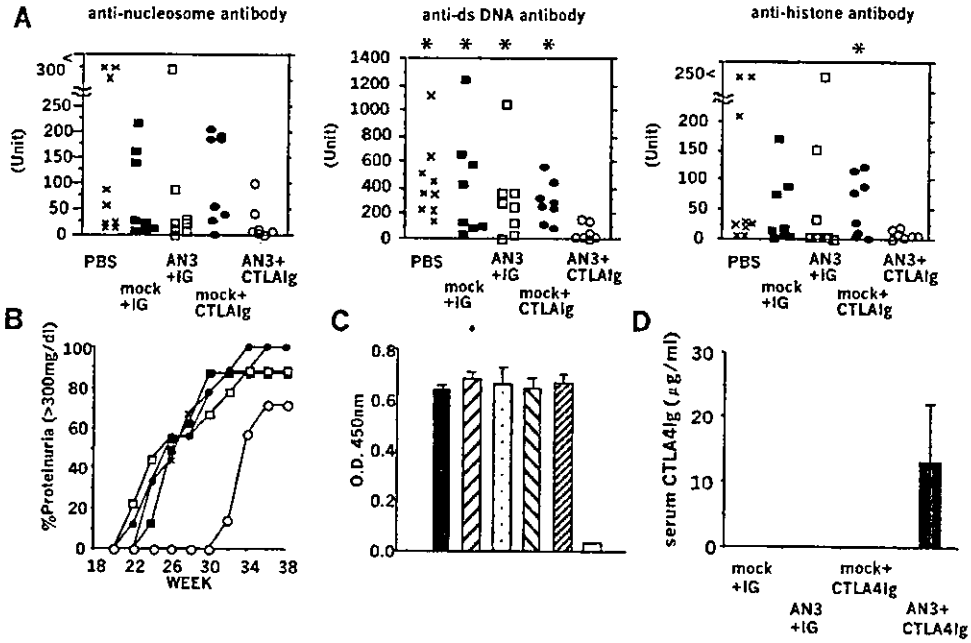

FIGURE 4. Effect of adoptively transferred engineered cells on disease progression. *A*, Suppression of autoantibody production. The elevation of serum anti-nucleosome, anti-dsDNA, and anti-histone Abs, measured by ELISA, was suppressed in AN3 + CTLA4Ig-injected mice at 22 wk. Statistically significant differences between AN3 + CTLA4Ig and control groups are denoted by asterisks ($p < 0.05$); $n = 7$ for AN3 + CTLA4Ig, and $n = 8$ for each control group. *B*, Cumulative percentage of mice in each group that developed severe proteinuria (>300 mg/dl). AN3 + CTLA4Ig showed suppressed progression of proteinuria compared with the control groups. x, PBS; ■, mock + IG; □, AN3 + IG; ●, mock + CTLA4Ig; ○, AN3 + CTLA4Ig. AN3 + CTLA4Ig vs the controls at 30 wk was significant ($p < 0.05$). *C*, A T cell-dependent humoral immune response to active immunization of OVA. Mice transferred with the engineered T cells at 10 wk of age were immunized with OVA in the footpad at 14 wk of age. Anti-OVA IgG Ab titer was measured at 17 wk of age. ■, PBS; ▨, mock + IG; ▩, AN3 + IG; ▧, mock + CTLA4Ig; ▨, AN3 + CTLA4Ig; □, no immunization. $n = 6$/group. *D*, Measurement of serum CTLA4Ig protein in the experimental groups with ELISA. Only AN3 + CTLA4Ig-transferred mice showed detectable, but low concentration of CTLA4Ig protein.